Supplemental Data Okuda et al., (2009) Pentatricopeptide repeat proteins with the DYW motif have distinct molecular functions in RNA editing and RNA cleavage in Arabidopsis chloroplasts.

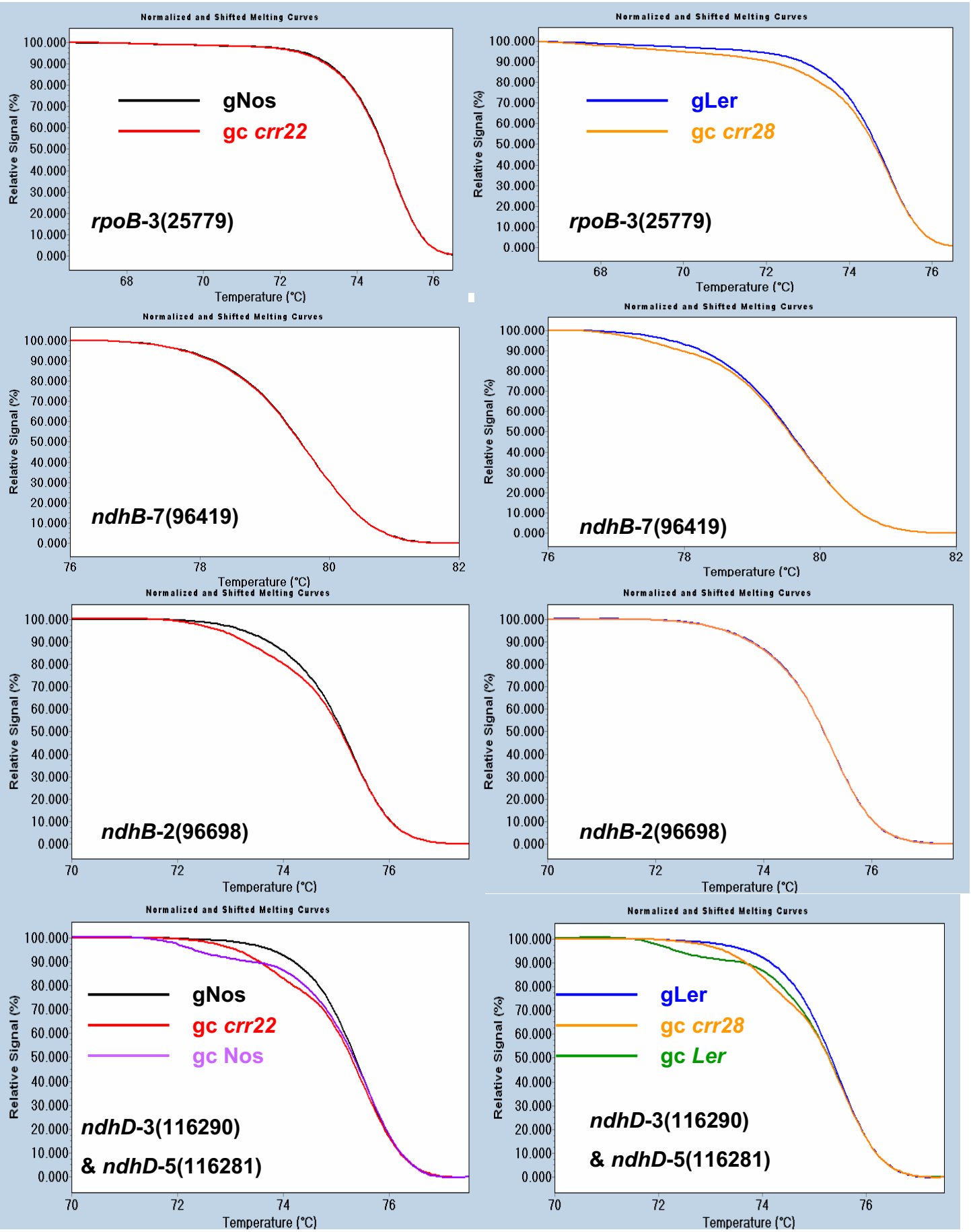

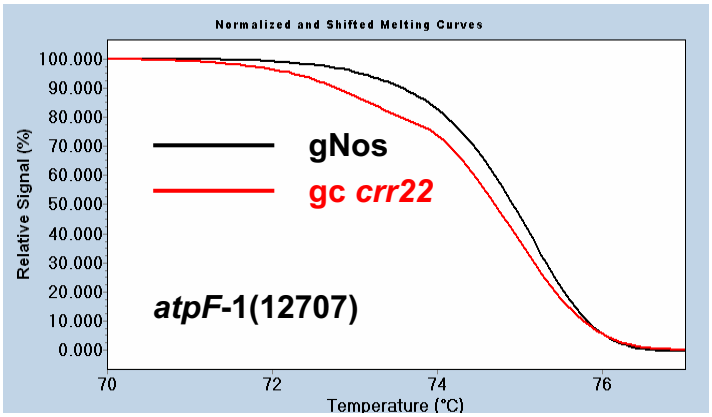
Normalized and Shifted Melting Curves
Relative Signal (%)
100.000
90.000
80.000
70.000
60.000
50.000
40.000
30.000
20.000
10.000
0.000
70
72
74
76
Temperature (°C)
gNos
gc crr22
atpF-1(12707)

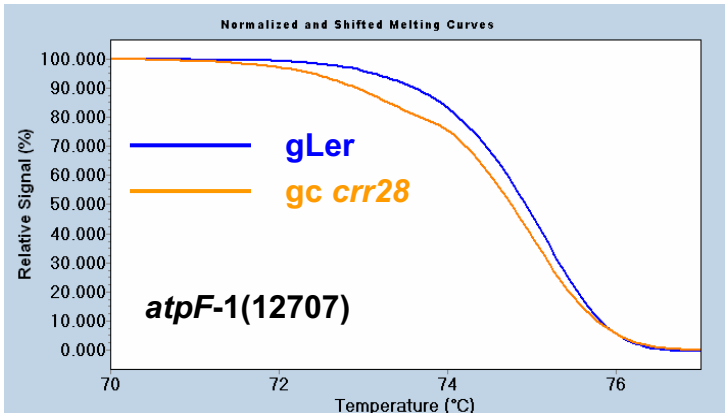
Normalized and Shifted Melting Curves
Relative Signal (%)
100.000
90.000
80.000
70.000
60.000
50.000
40.000
30.000
20.000
10.000
0.000
70
72
74
76
Temperature (°C)
gLer
gc crr28
atpF-1(12707)

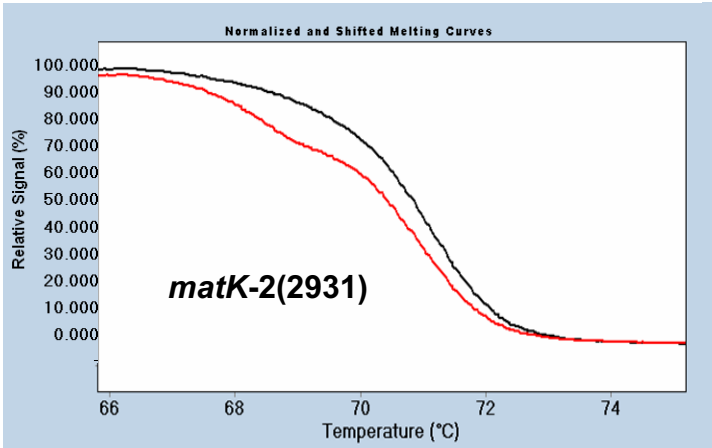
Normalized and Shifted Melting Curves
Relative Signal (%)
100.000
90.000
80.000
70.000
60.000
50.000
40.000
30.000
20.000
10.000
0.000
66
68
70
72
74
Temperature (°C)
matK-2(2931)

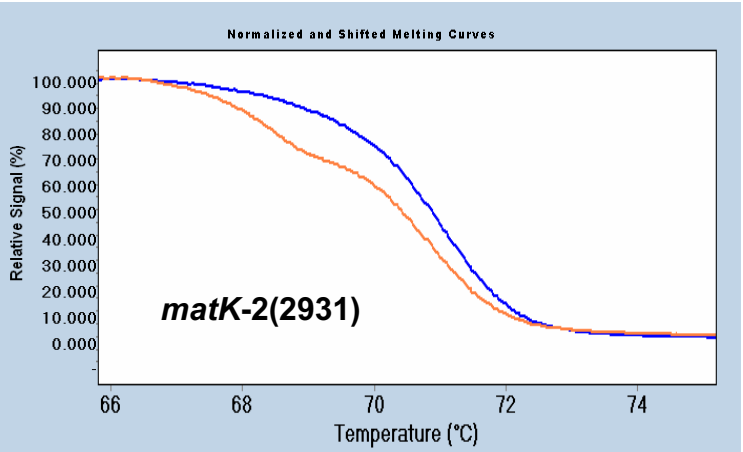
Normalized and Shifted Melting Curves
Relative Signal (%)
100.000
90.000
80.000
70.000
60.000
50.000
40.000
30.000
20.000
10.000
0.000
66
68
70
72
74
Temperature (°C)
matK-2(2931)

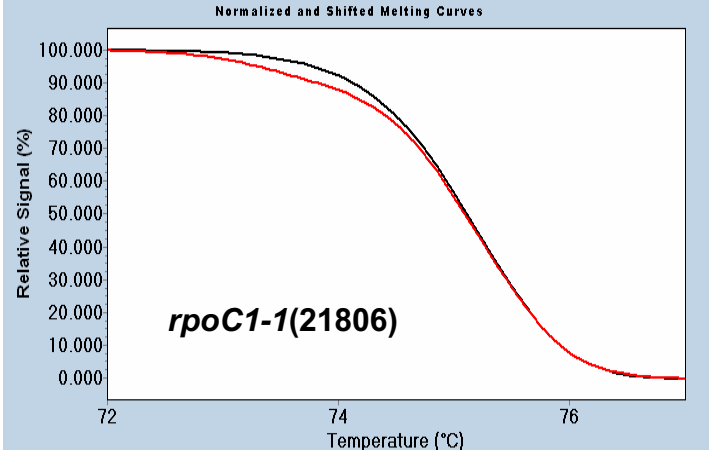
Normalized and Shifted Melting Curves
Relative Signal (%)
100.000
90.000
80.000
70.000
60.000
50.000
40.000
30.000
20.000
10.000
0.000
72
74
76
Temperature (°C)
rpoC1-1(21806)

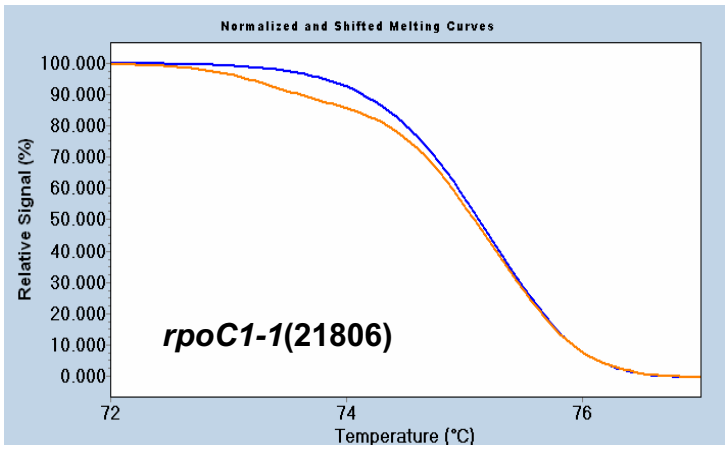
Normalized and Shifted Melting Curves
Relative Signal (%)
100.000
90.000
80.000
70.000
60.000
50.000
40.000
30.000
20.000
10.000
0.000
72
74
76
Temperature (°C)
rpoC1-1(21806)

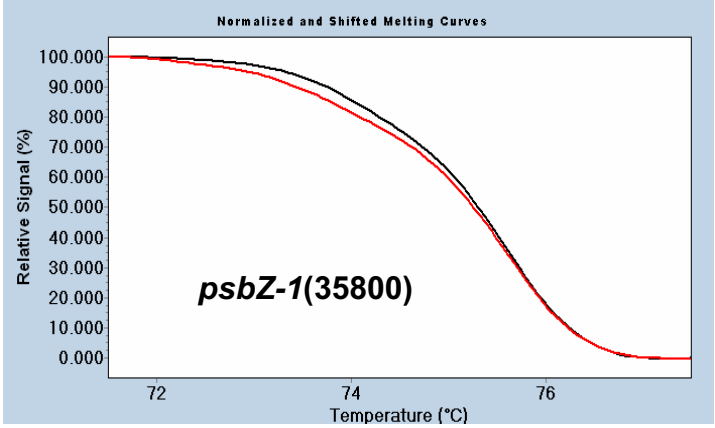
Normalized and Shifted Melting Curves
Relative Signal (%)
100.000
90.000
80.000
70.000
60.000
50.000
40.000
30.000
20.000
10.000
0.000
72
74
76
Temperature (°C)
psbZ-1(35800)

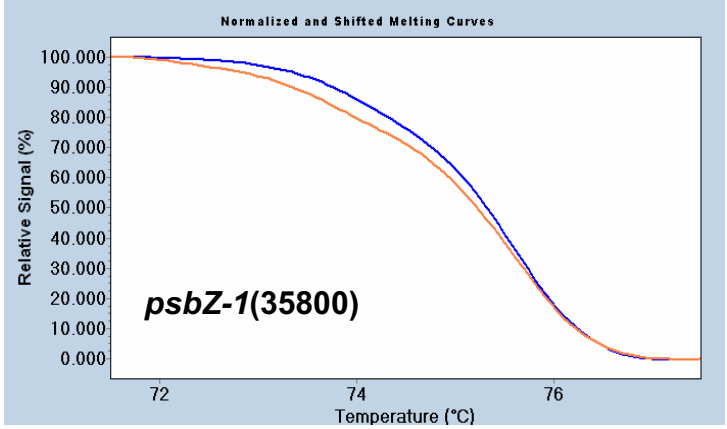
Normalized and Shifted Melting Curves
Relative Signal (%)
100.000
90.000
80.000
70.000
60.000
50.000
40.000
30.000
20.000
10.000
0.000
72
74
76
Temperature (°C)
psbZ-1(35800)

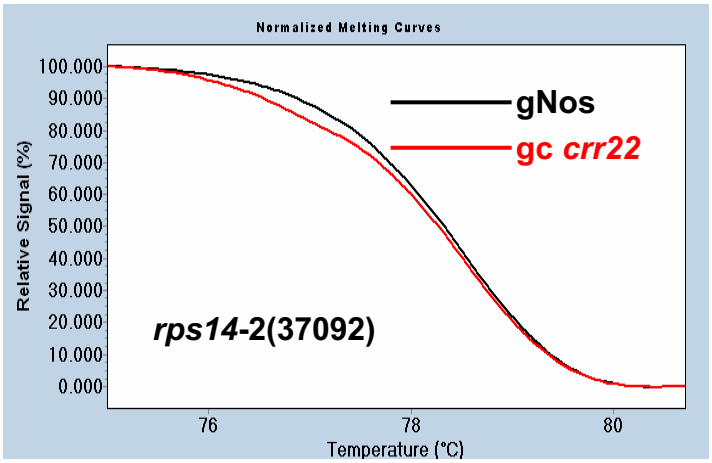
Normalized Melting Curves
Relative Signal (%)
100.000
90.000
80.000
70.000
60.000
50.000
40.000
30.000
20.000
10.000
0.000
76
78
80
Temperature (°C)
gNos
gc crr22
rps14-2(37092)

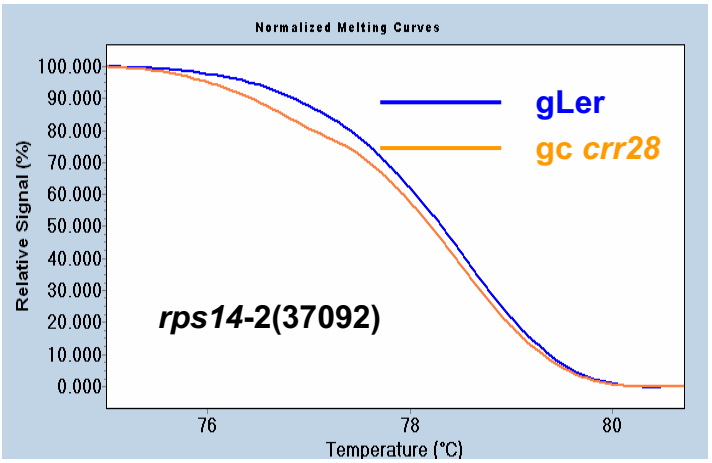
Normalized Melting Curves
Relative Signal (%)
100.000
90.000
80.000
70.000
60.000
50.000
40.000
30.000
20.000
10.000
0.000
76
78
80
Temperature (°C)
gLer
gc crr28
rps14-2(37092)

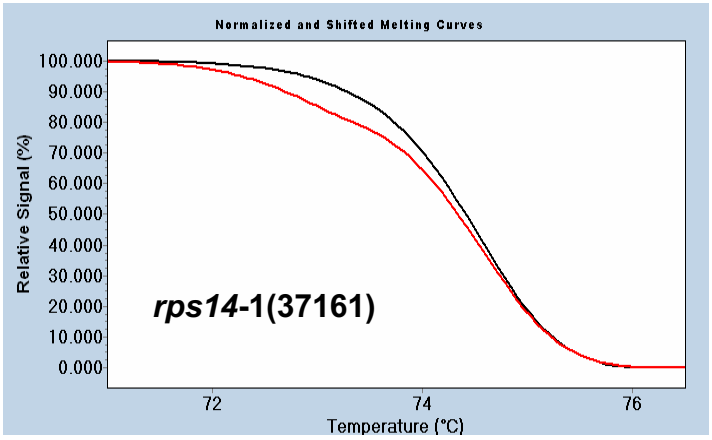
Normalized and Shifted Melting Curves
Relative Signal (%)
100.000
90.000
80.000
70.000
60.000
50.000
40.000
30.000
20.000
10.000
0.000
72
74
76
Temperature (°C)
rps14-1(37161)

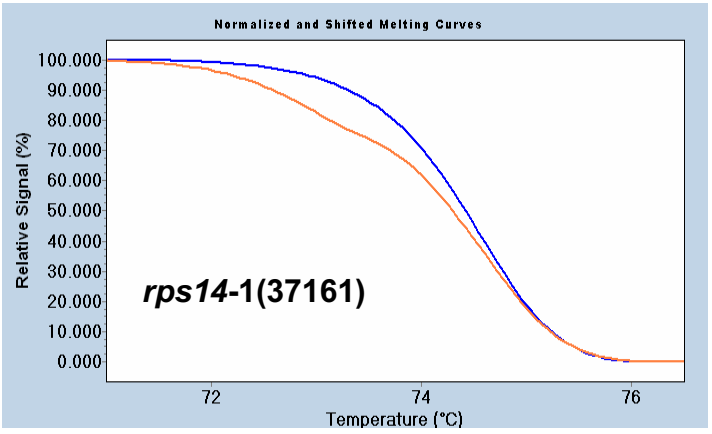
Normalized and Shifted Melting Curves
Relative Signal (%)
100.000
90.000
80.000
70.000
60.000
50.000
40.000
30.000
20.000
10.000
0.000
72
74
76
Temperature (°C)
rps14-1(37161)

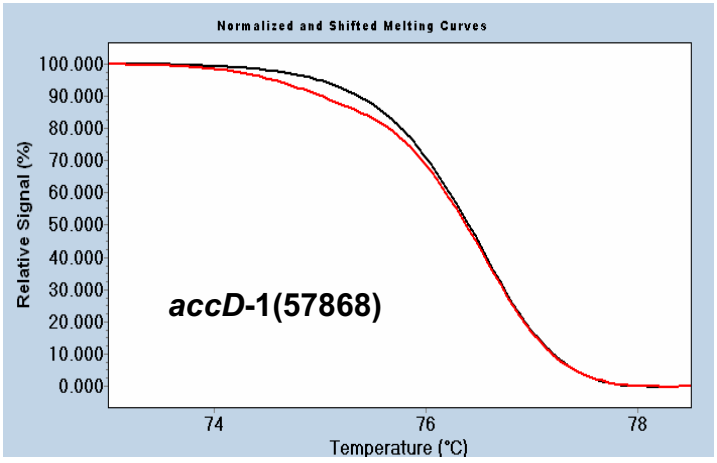
Normalized and Shifted Melting Curves
Relative Signal (%)
100.000
90.000
80.000
70.000
60.000
50.000
40.000
30.000
20.000
10.000
0.000
74
76
78
Temperature (°C)
accD-1(57868)

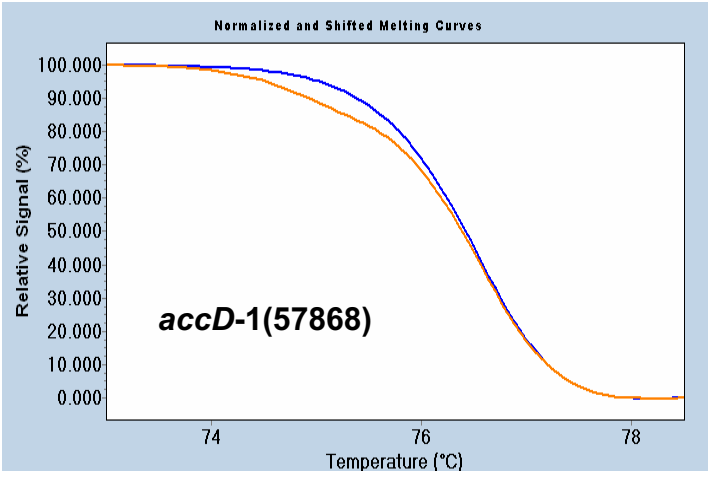
Normalized and Shifted Melting Curves
Relative Signal (%)
100.000
90.000
80.000
70.000
60.000
50.000
40.000
30.000
20.000
10.000
0.000
74
76
78
Temperature (°C)
accD-1(57868)

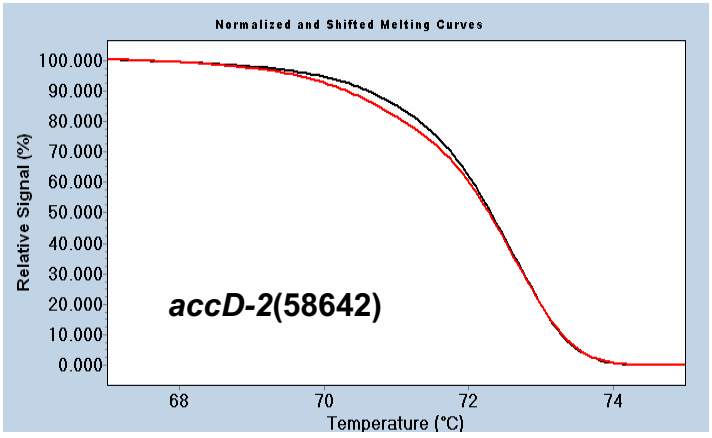
Normalized and Shifted Melting Curves
Relative Signal (%)
100.000
90.000
80.000
70.000
60.000
50.000
40.000
30.000
20.000
10.000
0.000
68
70
72
74
Temperature (°C)
accD-2(58642)

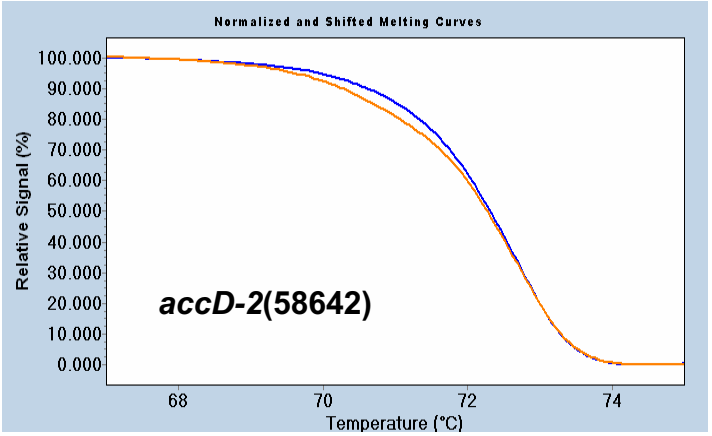
Normalized and Shifted Melting Curves
Relative Signal (%)
100.000
90.000
80.000
70.000
60.000
50.000
40.000
30.000
20.000
10.000
0.000
68
70
72
74
Temperature (°C)
accD-2(58642)

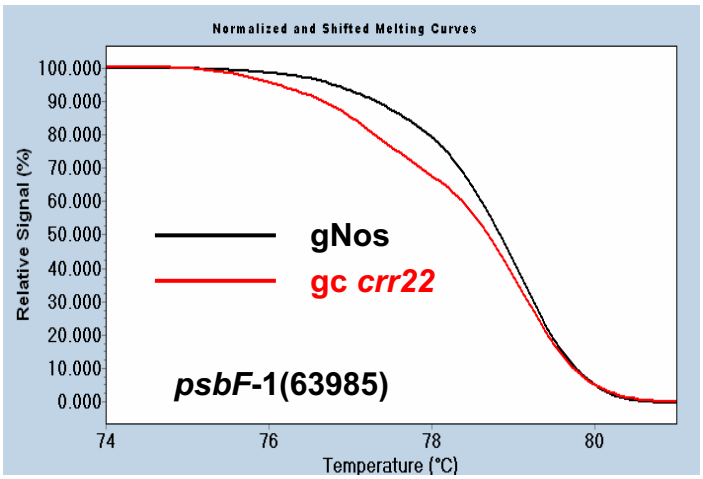
Normalized and Shifted Melting Curves
Relative Signal (%)
Temperature (°C)
gNos
gc crr22
psbF-1(63985)

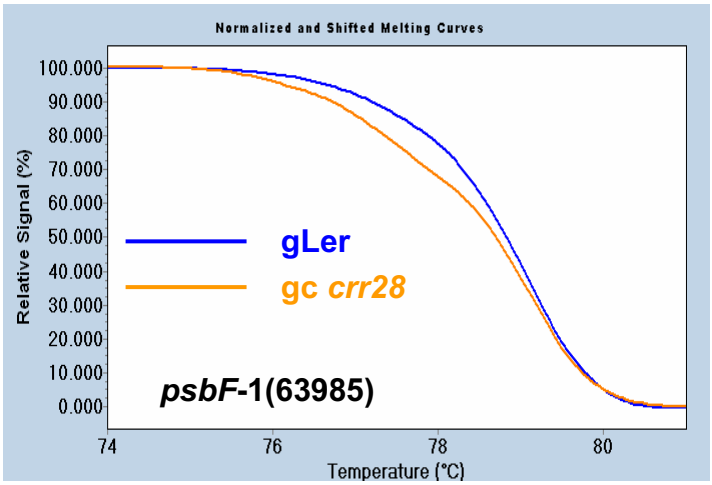
Normalized and Shifted Melting Curves
Relative Signal (%)
Temperature (°C)
gLer
gc crr28
psbF-1(63985)

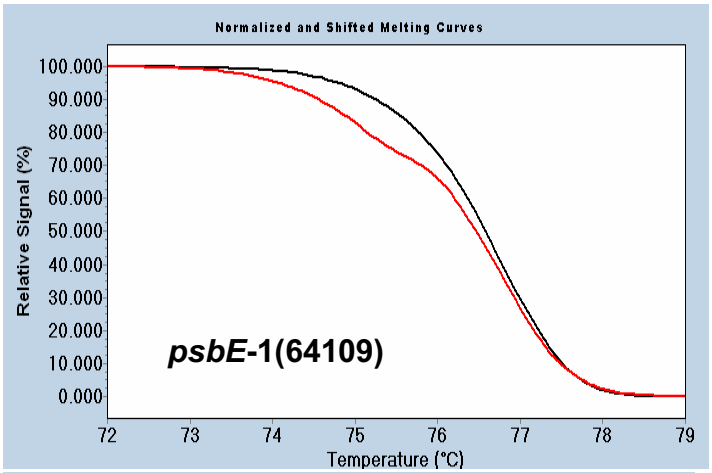
Normalized and Shifted Melting Curves
Relative Signal (%)
Temperature (°C)
psbE-1(64109)

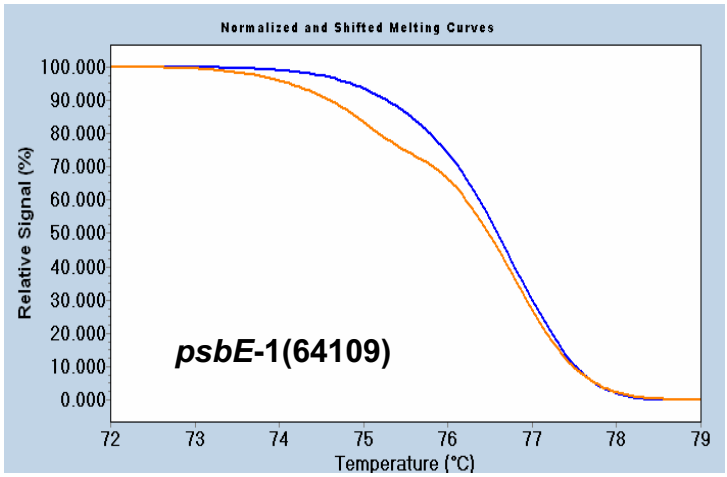
Normalized and Shifted Melting Curves
Relative Signal (%)
Temperature (°C)
psbE-1(64109)

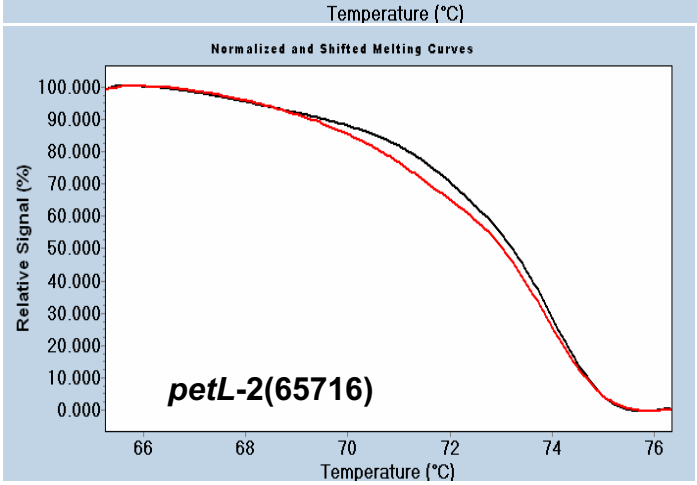
Normalized and Shifted Melting Curves
Relative Signal (%)
Temperature (°C)
petL-2(65716)

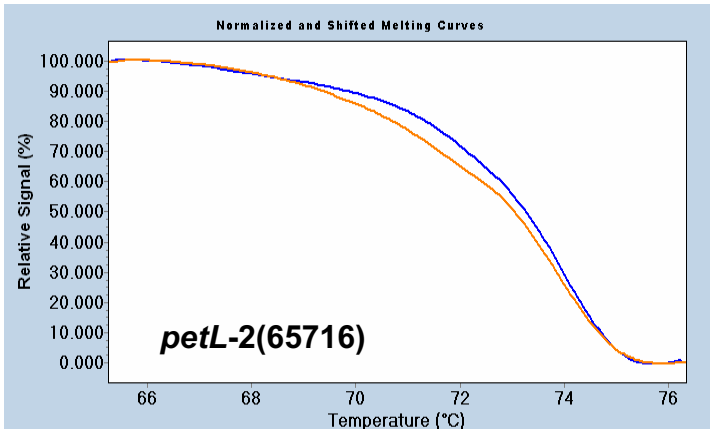
Normalized and Shifted Melting Curves
Relative Signal (%)
Temperature (°C)
petL-2(65716)

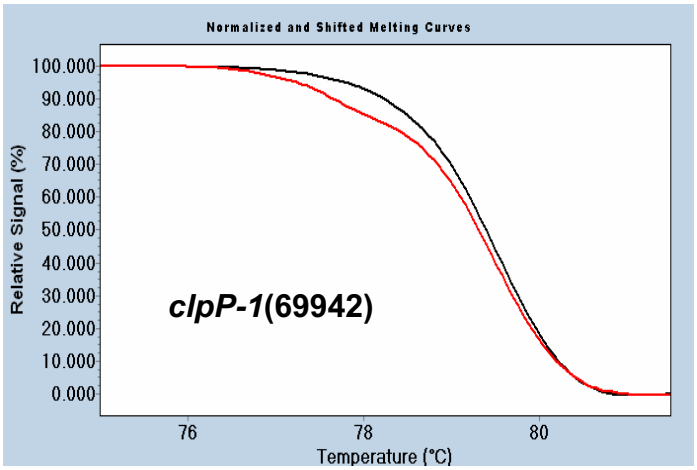
Normalized and Shifted Melting Curves
Relative Signal (%)
Temperature (°C)
clpP-1(69942)

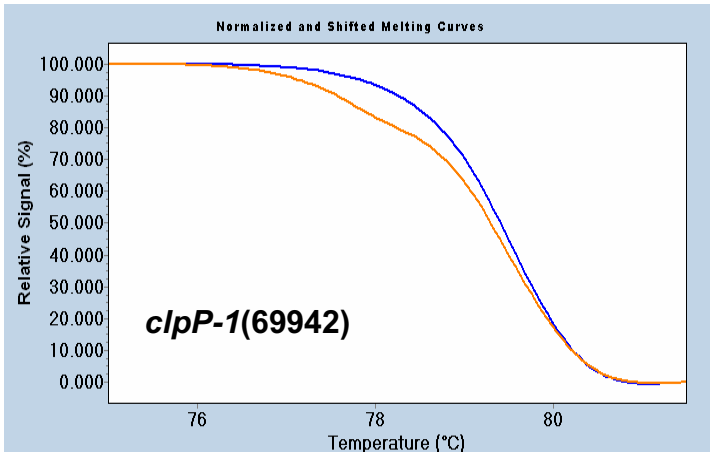
Normalized and Shifted Melting Curves
Relative Signal (%)
Temperature (°C)
clpP-1(69942)

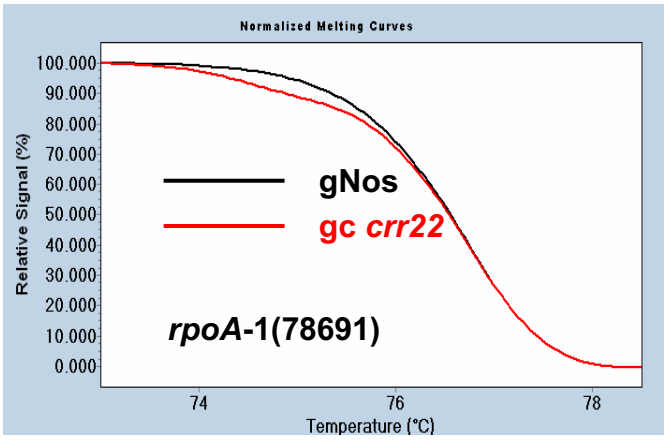
Normalized Melting Curves
Relative Signal (%)
Temperature (°C)
gNos
gc crr22
rpoA-1(78691)

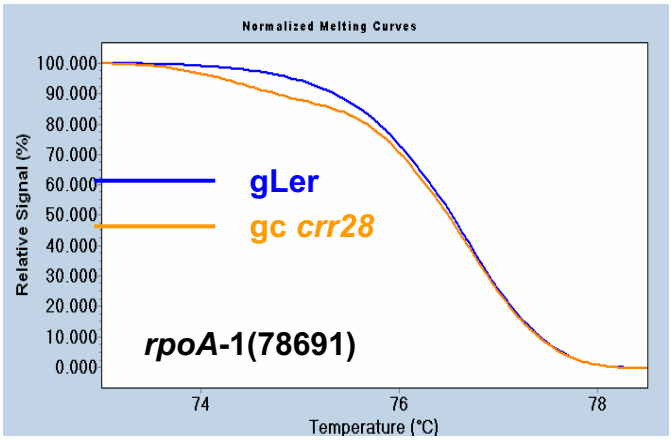
Normalized Melting Curves
Relative Signal (%)
Temperature (°C)
gLer
gc crr28
rpoA-1(78691)

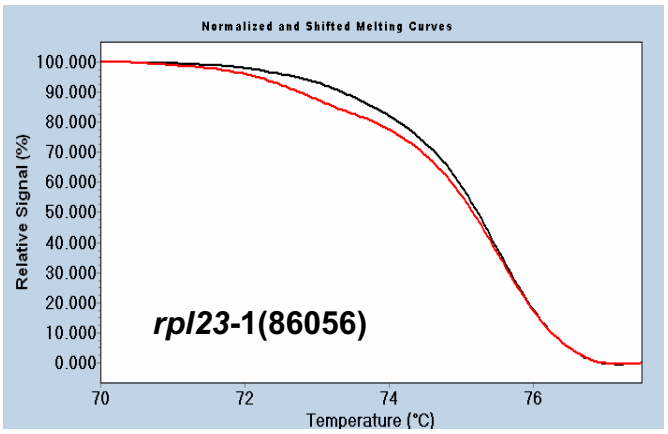
Normalized and Shifted Melting Curves
Relative Signal (%)
Temperature (°C)
rpl23-1(86056)

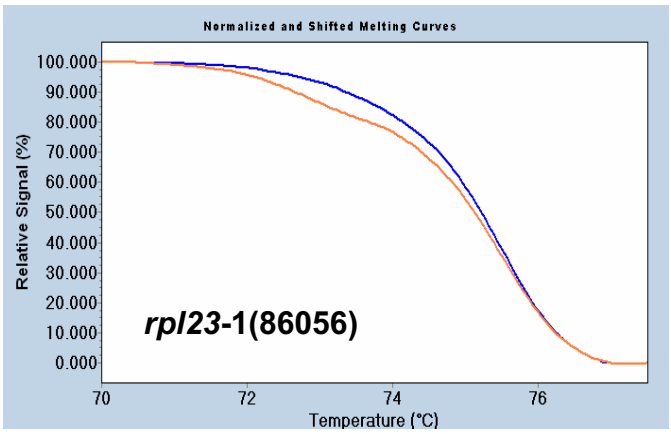
Normalized and Shifted Melting Curves
Relative Signal (%)
Temperature (°C)
rpl23-1(86056)

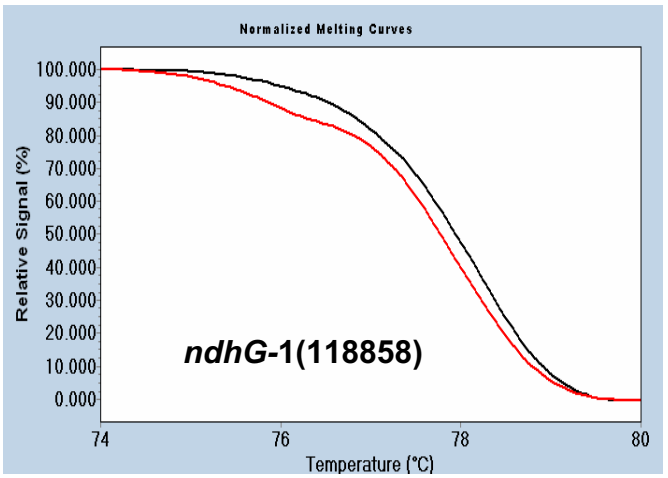
Normalized Melting Curves
Relative Signal (%)
Temperature (°C)
ndhG-1(118858)

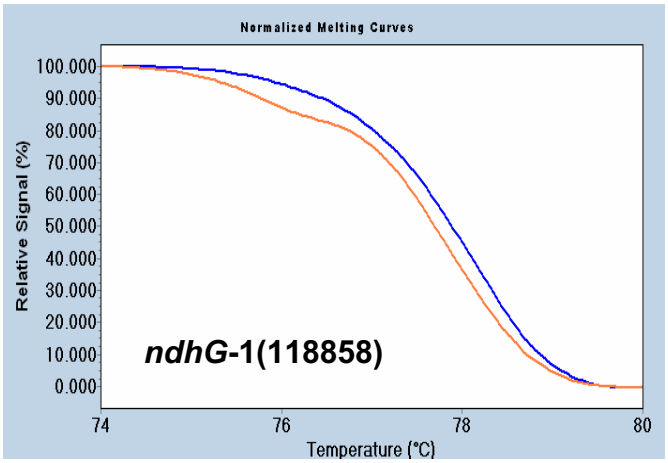
Normalized Melting Curves
Relative Signal (%)
Temperature (°C)
ndhG-1(118858)

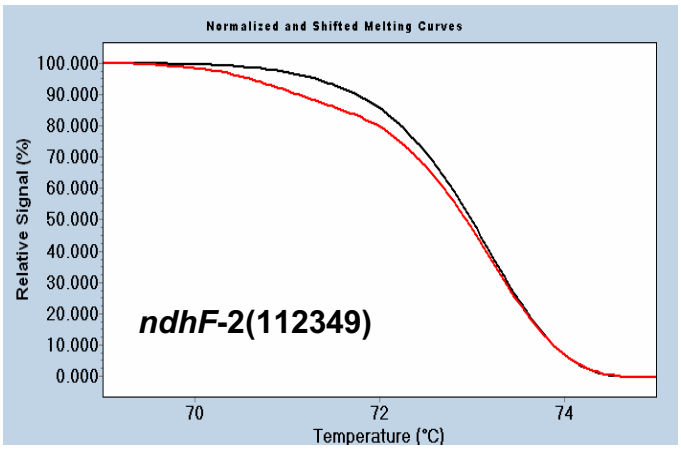
Normalized and Shifted Melting Curves
Relative Signal (%)
Temperature (°C)
ndhF-2(112349)

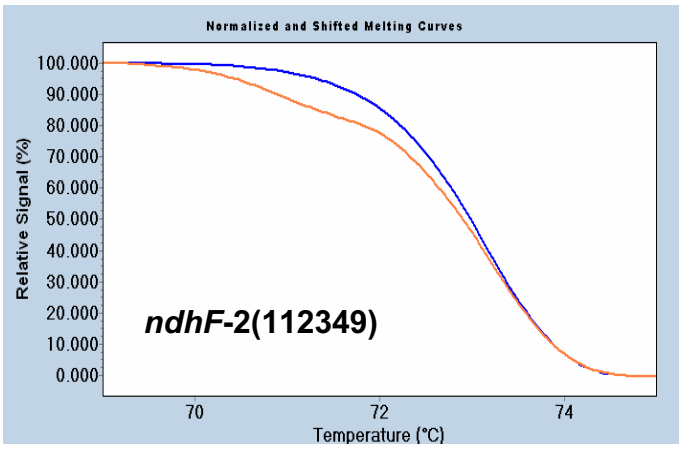
Normalized and Shifted Melting Curves
Relative Signal (%)
Temperature (°C)
ndhF-2(112349)

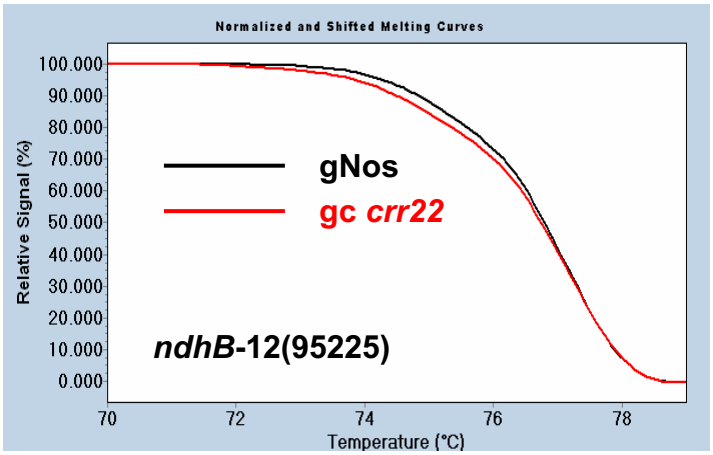
Normalized and Shifted Melting Curves
Relative Signal (%)
Temperature (°C)
gNos
gc crr22
ndhB-12(95225)

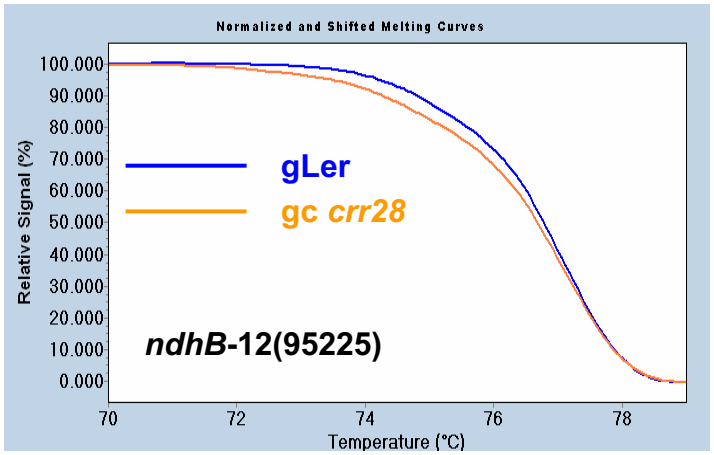
Normalized and Shifted Melting Curves
Relative Signal (%)
Temperature (°C)
gLer
gc crr28
ndhB-12(95225)

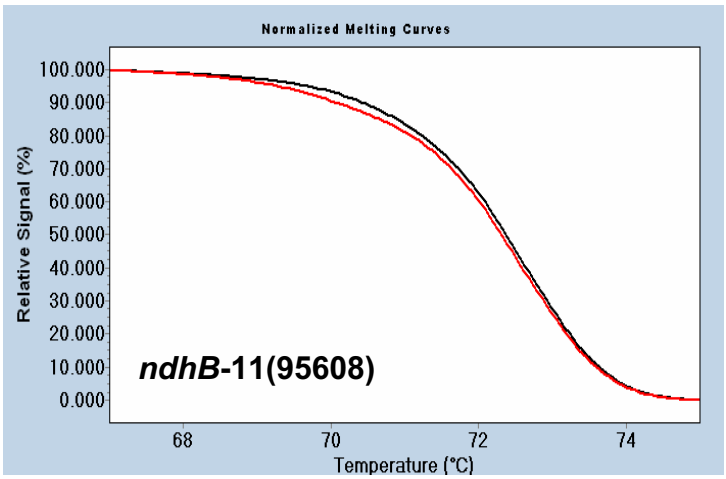
Normalized Melting Curves
Relative Signal (%)
Temperature (°C)
ndhB-11(95608)

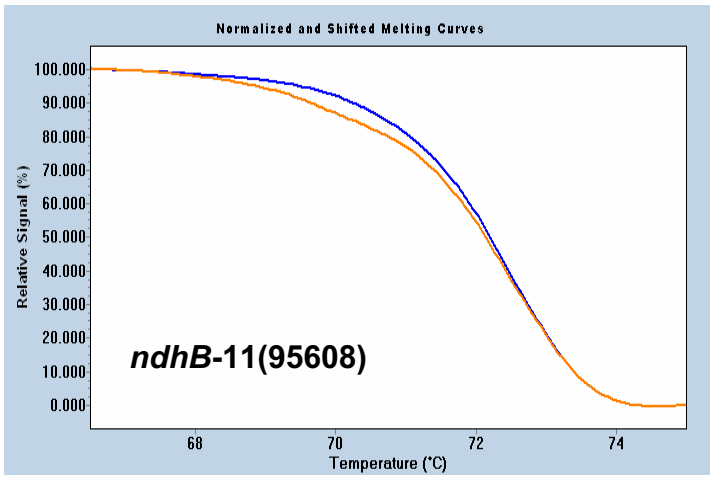
Normalized and Shifted Melting Curves
Relative Signal (%)
Temperature (°C)
ndhB-11(95608)

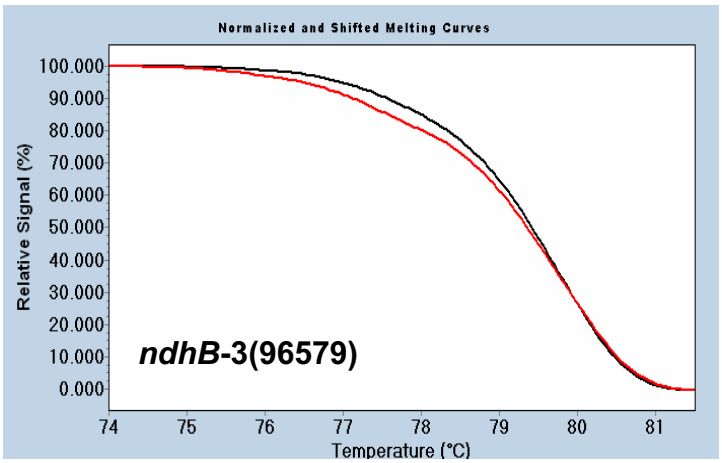
Normalized and Shifted Melting Curves
Relative Signal (%)
Temperature (°C)
ndhB-3(96579)

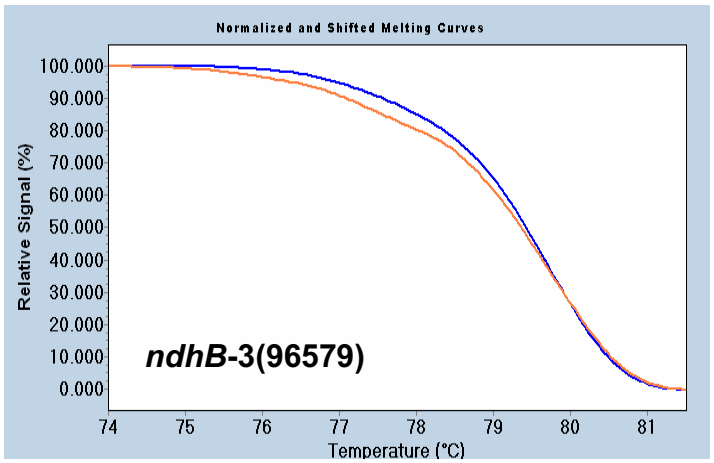
Normalized and Shifted Melting Curves
Relative Signal (%)
Temperature (°C)
ndhB-3(96579)

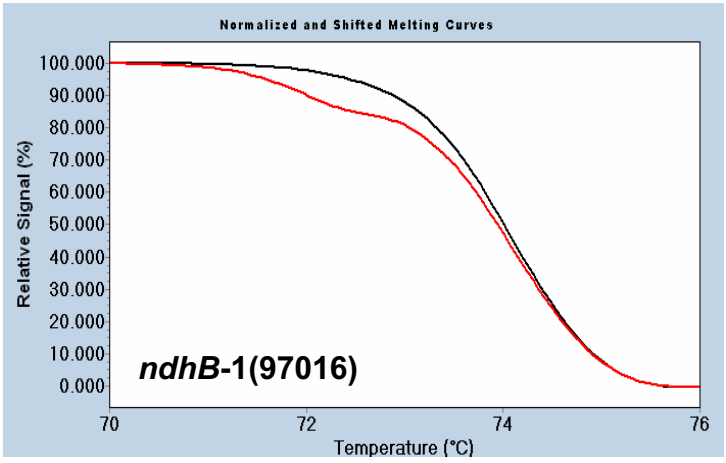
Normalized and Shifted Melting Curves
Relative Signal (%)
Temperature (°C)
ndhB-1(97016)

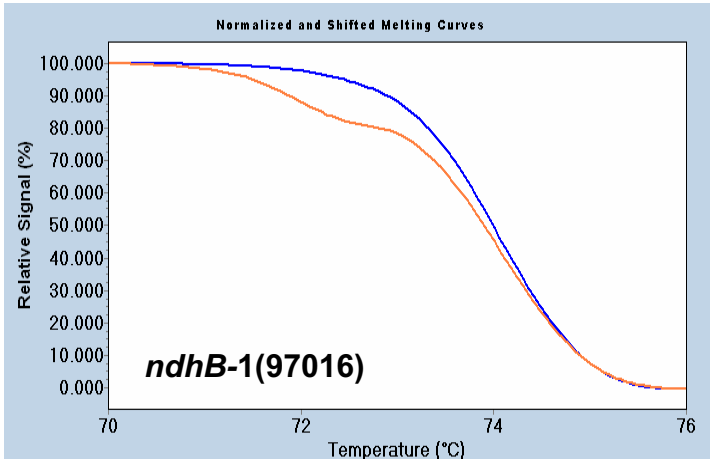
Normalized and Shifted Melting Curves
Relative Signal (%)
Temperature (°C)
ndhB-1(97016)

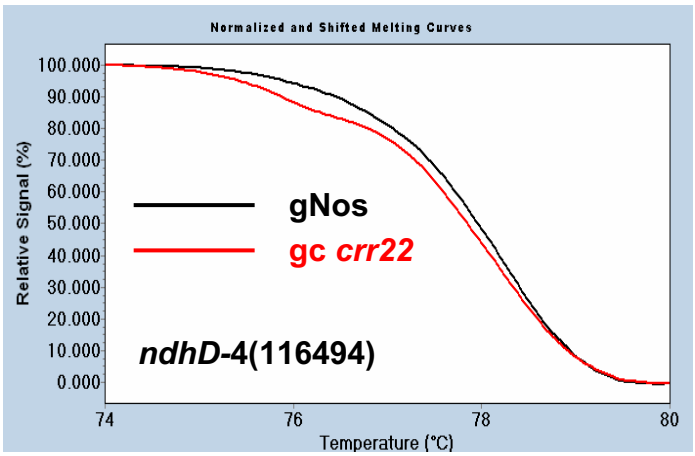
Normalized and Shifted Melting Curves
Relative Signal (%)
100.000
90.000
80.000
70.000
60.000
50.000
40.000
30.000
20.000
10.000
0.000
74
76
78
80
Temperature (°C)
gNos
gc crr22
ndhD-4(116494)

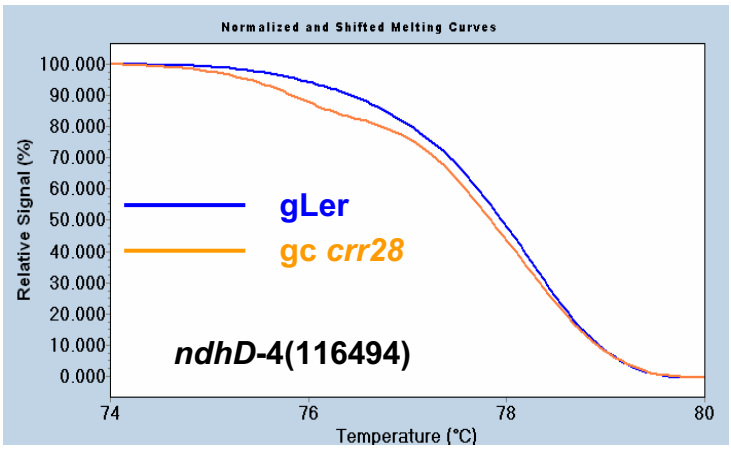
Normalized and Shifted Melting Curves
Relative Signal (%)
100.000
90.000
80.000
70.000
60.000
50.000
40.000
30.000
20.000
10.000
0.000
74
76
78
80
Temperature (°C)
gLer
gc crr28
ndhD-4(116494)

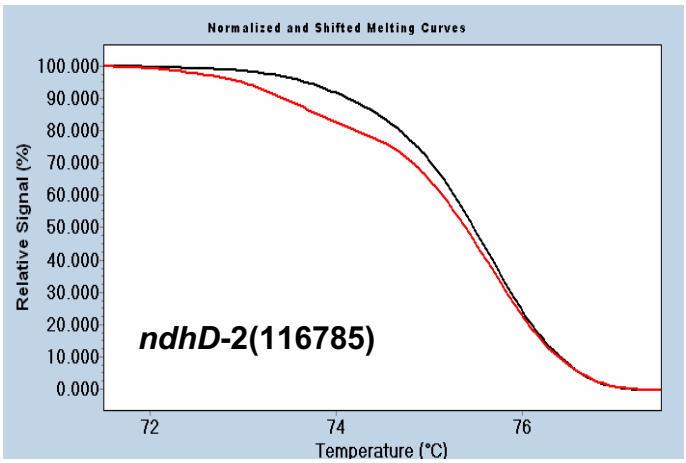
Normalized and Shifted Melting Curves
Relative Signal (%)
100.000
90.000
80.000
70.000
60.000
50.000
40.000
30.000
20.000
10.000
0.000
72
74
76
Temperature (°C)
ndhD-2(116785)

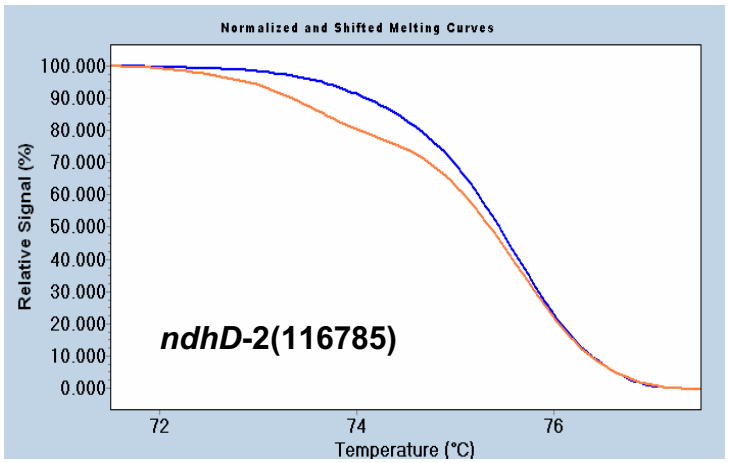
Normalized and Shifted Melting Curves
Relative Signal (%)
100.000
90.000
80.000
70.000
60.000
50.000
40.000
30.000
20.000
10.000
0.000
72
74
76
Temperature (°C)
ndhD-2(116785)

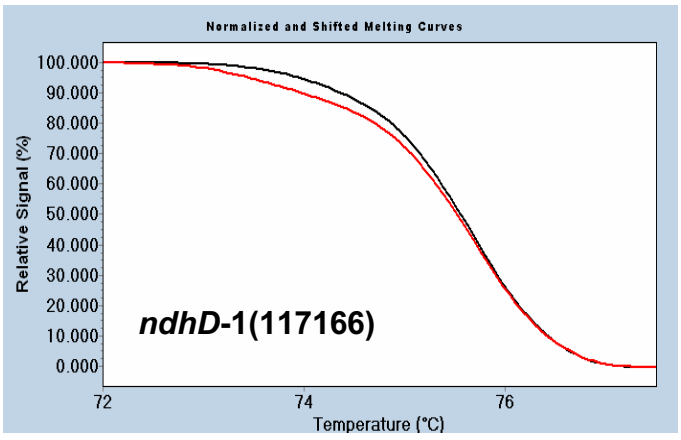
Normalized and Shifted Melting Curves
Relative Signal (%)
100.000
90.000
80.000
70.000
60.000
50.000
40.000
30.000
20.000
10.000
0.000
72
74
76
Temperature (°C)
ndhD-1(117166)

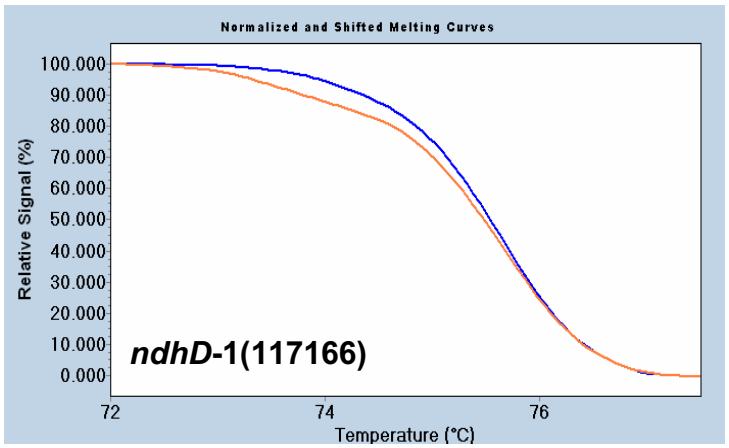
Normalized and Shifted Melting Curves
Relative Signal (%)
100.000
90.000
80.000
70.000
60.000
50.000
40.000
30.000
20.000
10.000
0.000
72
74
76
Temperature (°C)
ndhD-1(117166)

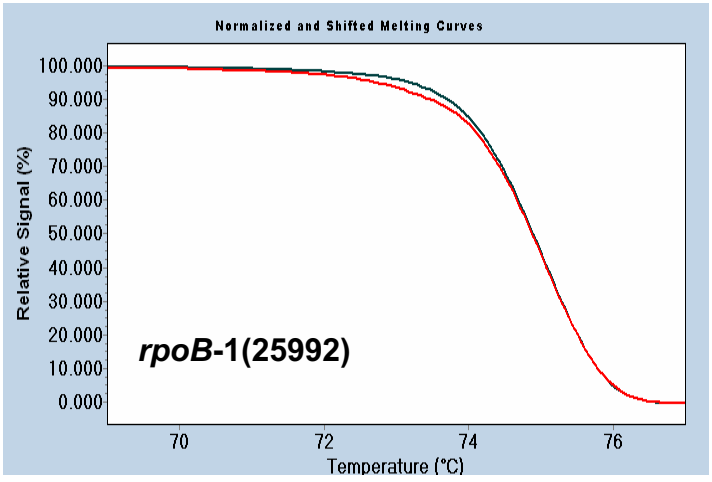
Normalized and Shifted Melting Curves
Relative Signal (%)
100.000
90.000
80.000
70.000
60.000
50.000
40.000
30.000
20.000
10.000
0.000
70
72
74
76
Temperature (°C)
rpoB-1(25992)

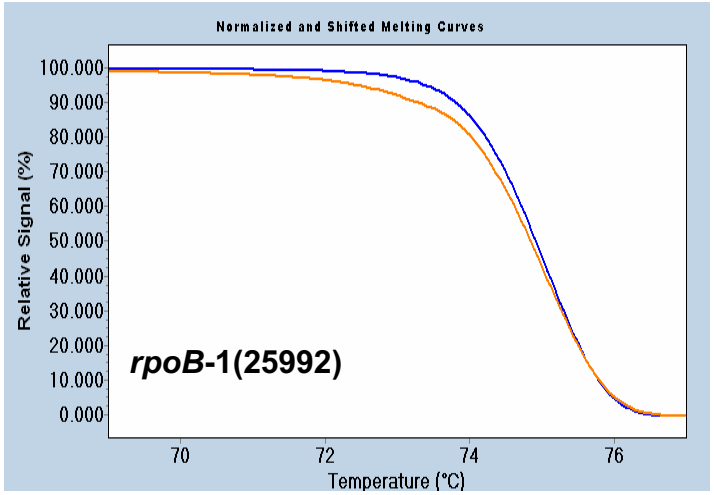
Normalized and Shifted Melting Curves
Relative Signal (%)
100.000
90.000
80.000
70.000
60.000
50.000
40.000
30.000
20.000
10.000
0.000
70
72
74
76
Temperature (°C)
rpoB-1(25992)

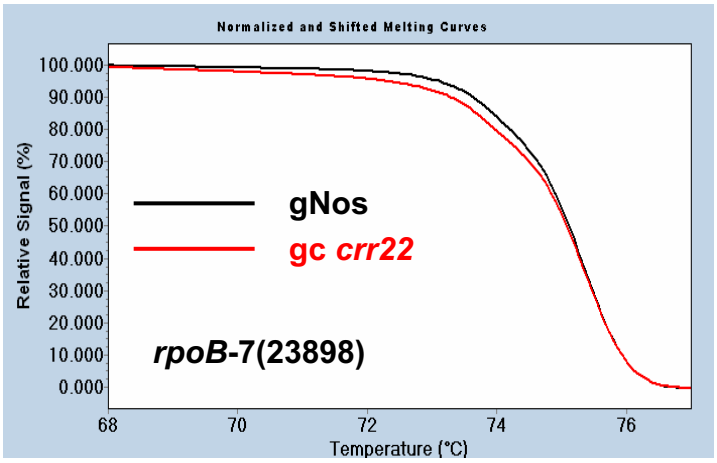
Normalized and Shifted Melting Curves
Relative Signal (%)
Temperature (°C)
gNos
gc crr22
rpoB-7(23898)

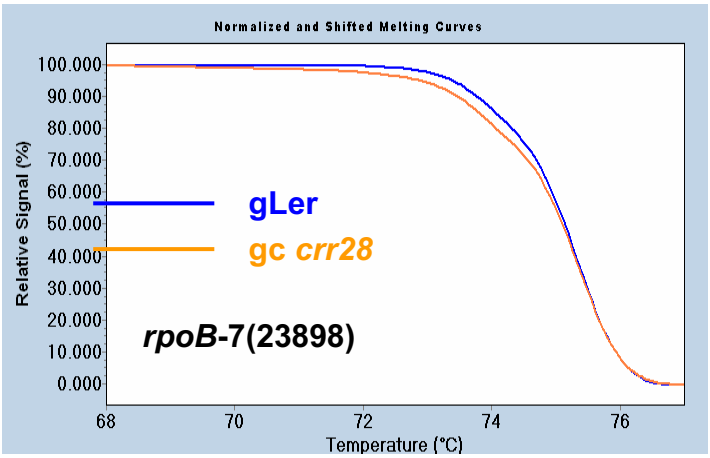
Normalized and Shifted Melting Curves
Relative Signal (%)
Temperature (°C)
gLer
gc crr28
rpoB-7(23898)

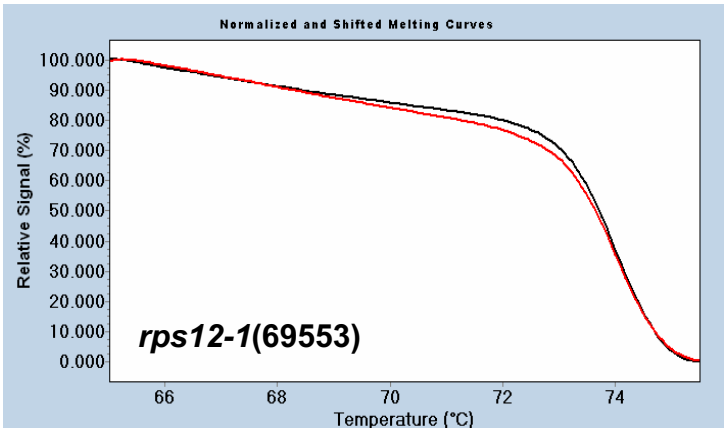
Normalized and Shifted Melting Curves
Relative Signal (%)
Temperature (°C)
rps12-1(69553)

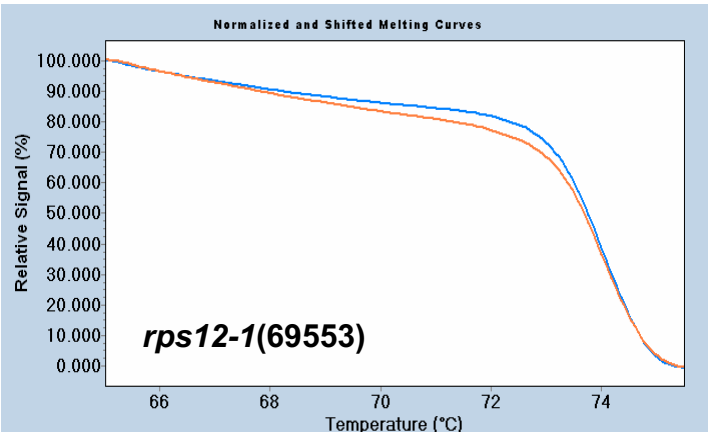
Normalized and Shifted Melting Curves
Relative Signal (%)
Temperature (°C)
rps12-1(69553)

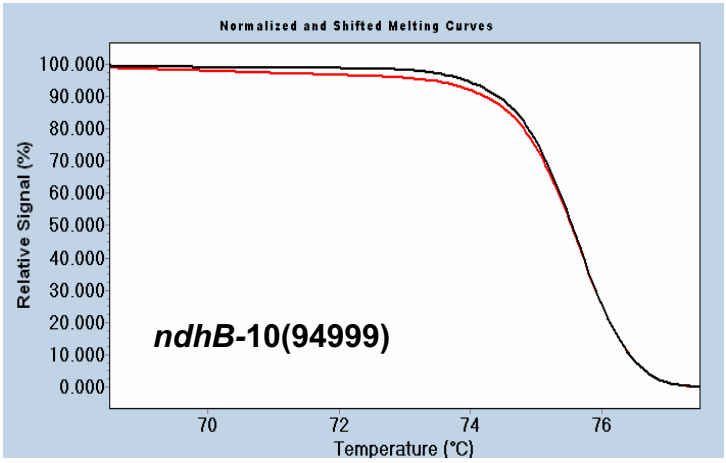
Normalized and Shifted Melting Curves
Relative Signal (%)
Temperature (°C)
ndhB-10(94999)

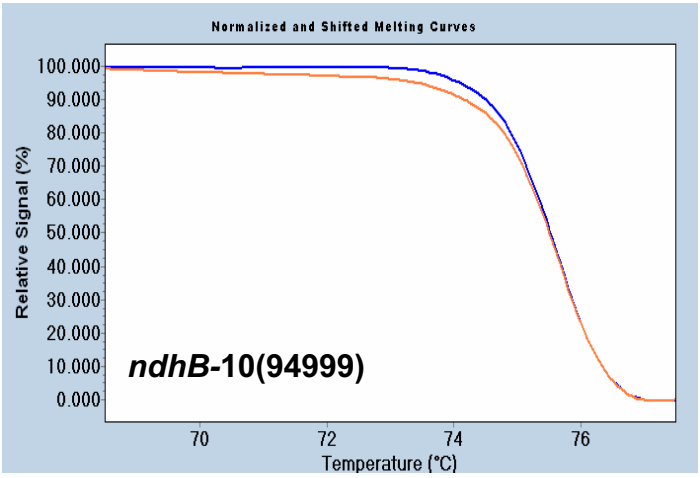
Normalized and Shifted Melting Curves
Relative Signal (%)
Temperature (°C)
ndhB-10(94999)

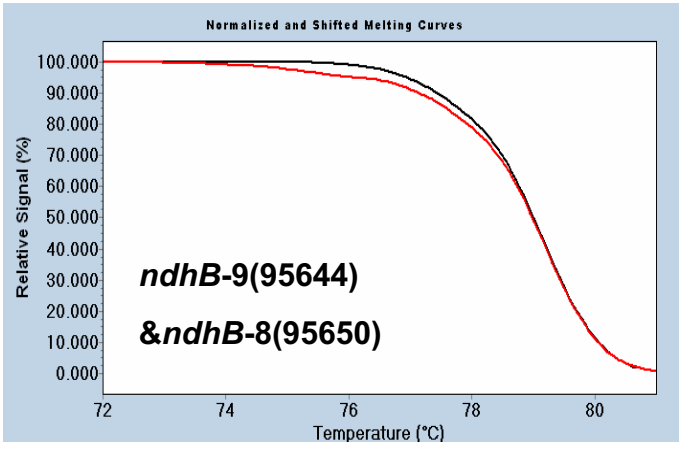
Normalized and Shifted Melting Curves
Relative Signal (%)
Temperature (°C)
ndhB-9(95644)
&ndhB-8(95650)

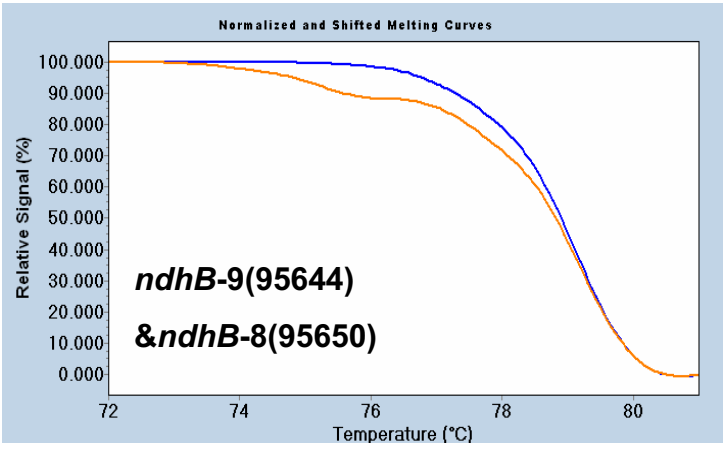
Normalized and Shifted Melting Curves
Relative Signal (%)
Temperature (°C)
ndhB-9(95644)
&ndhB-8(95650)

Supplemental Figure 1. High resolution melting screen of *crr22* and *crr28* mutants. Real-time PCR was done using primers surrounding the 34 known editing sites of *Arabidopsis* in the presence of a fluorescent double-strand-specific dye. At the end of the amplification, amplicons were denatured, renatured and then melted using precise incremental increases in temperature. Melting of DNA duplexes releases the dye, causing a decrease in fluorescence. The presence of less thermostable heteroduplexes in a sample alters the shape of the melting curves. For each editing site, the melting curve of a control consisting of genomic DNA (g) from the wt sample was compared to the melting curves of a mix of genomic DNA and cDNA (gc) from the mutant lines. Editing produces cDNA with a nucleotide change and thus the mix of genomic DNA and cDNA exhibits a different melting curve from that of genomic DNA alone. If an editing site is unedited in the mutant, then the melting curves from the genomic DNA sample and the mixed genomic/cDNA sample are identical.

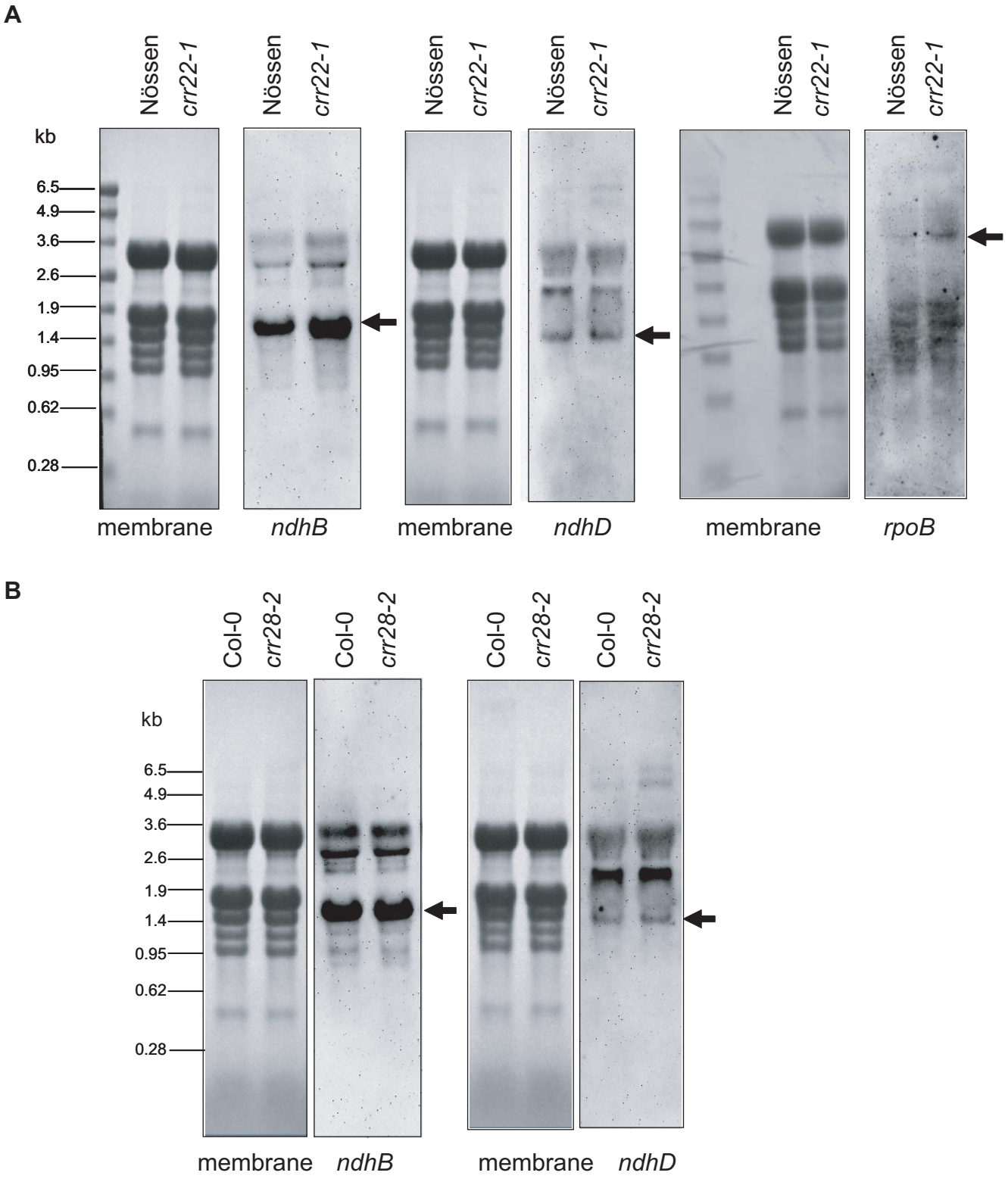

Supplemental Figure 2. Transcript profiles of genes with editing defects in *crr22* (A) and *crr28* (B). Ten µg of RNA from 15-day-old seedlings (15 µg for *rpoB*) was loaded on formaldehyde agarose gels and transferred onto a membrane. Hybridizations were performed under high-stringency conditions using antisense RNA probes for the genes specified for each blot. The arrows point at the mature transcript. The sizes of

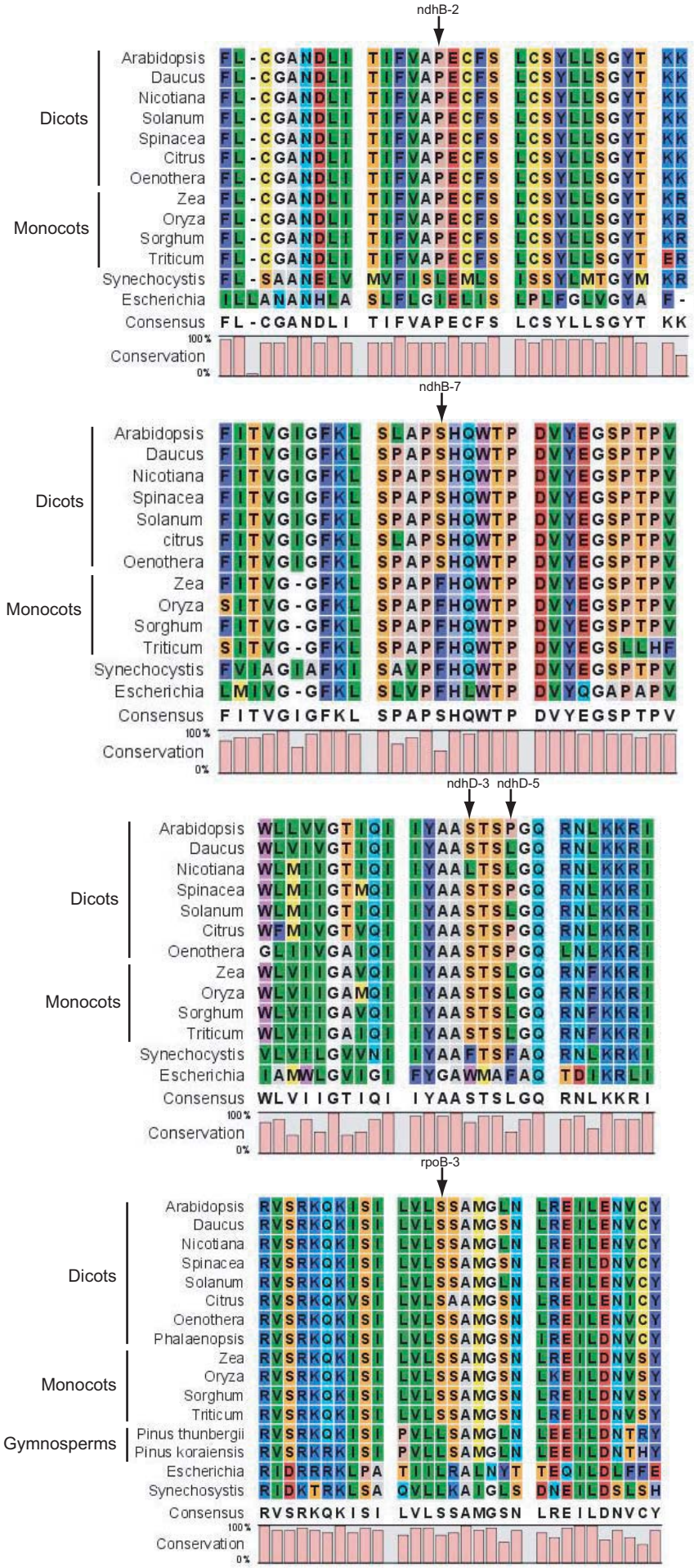

Supplemental Figure 3. Partial sequence alignments of NdhB, NdhD, and RpoB around the amino acids affected by RNA editing. *Arabidopsis* NdhB, NdhD, and RpoB proteins were aligned with their homologues from other species. The alignment was performed by using CLC Free Workbench 3.1 software (http://www.clcbio.com)

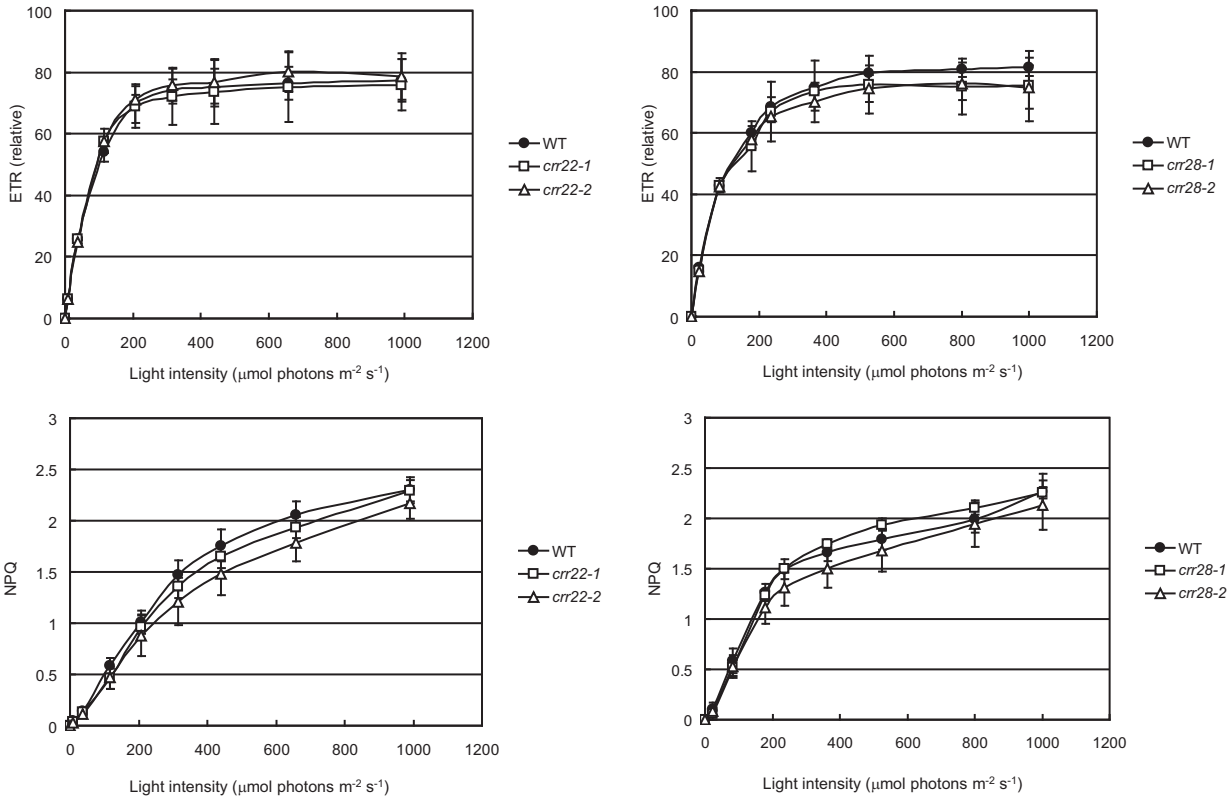

Supplemental Figure 4. *In vivo* analysis of electron transport activity. (A) Light intensity dependence of ETR (electron transport rate). ETR is plotted relative to ϕ_{PSII} × light intensity (μmol photons m^{-2} s^{-1}), where ϕ_{PSII} is quantum yield of photosystem II **(B)** Light intensity dependence of NPQ (non-photochemical quenching) of chlorophyll fluorescence. All values represent the mean ±SD (n=3).

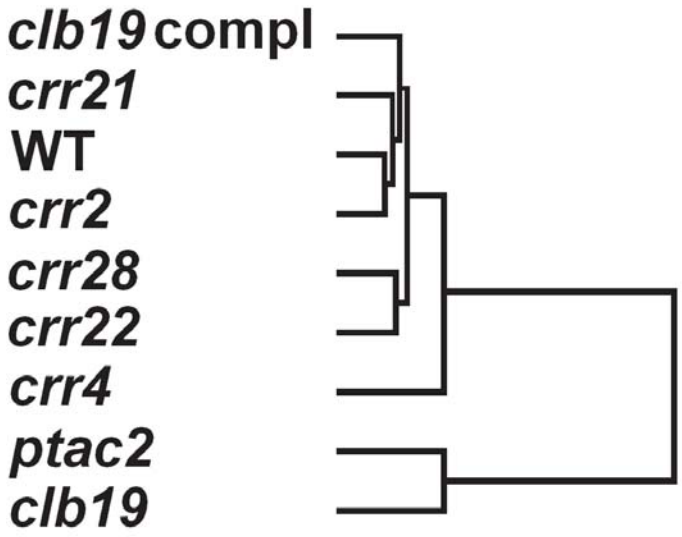

Supplemental Figure 5. Hierarchical clustering of *crr22* and *crr28* mutants based on their plastid RNA profiles assessed by quantitative RT-PCR. The tree was calculated using the euclidian distance based on $\log_2$ (mutant/WT) ratios for all plastid transcripts. *clb19* (Chateigner-Boutin et al., 2008) and *ptac2* (Pfalz et al., 2006) are impaired in PEP activity and *otp51* (de Longevialle et al., 2008) shows a specific *ycf3* splicing defect.

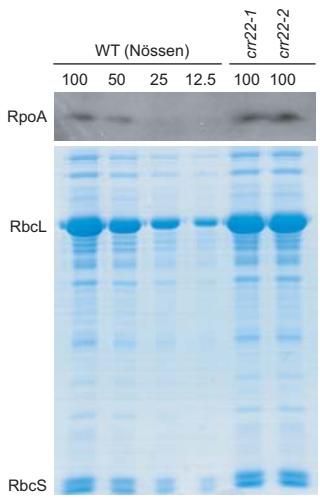

Supplemental Figure 6. Protein blot analysis of the plastid-encoded RNA polymerase (PEP). Immunodetection was performed using antibodies against the PEP subunit, RpoA. Proteins were extracted from the stroma fraction. The lanes were loaded with protein samples corresponding to 1.0 µg chlorophyll for RpoA (100%) and the series of dilutions indicated. The Coomassie Brilliant Blue stained gel lanes are shown as loading controls.

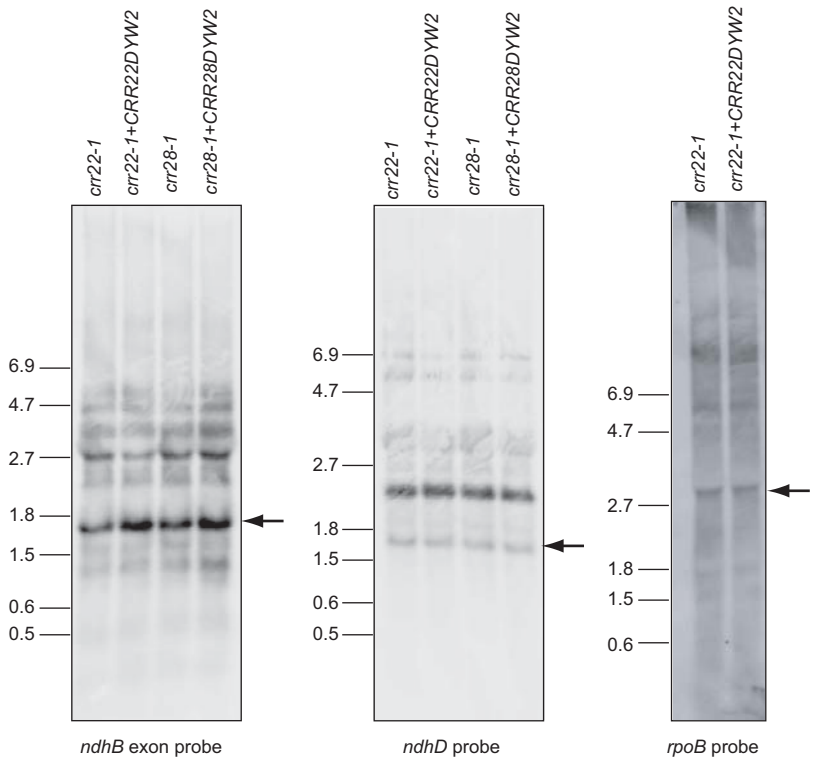

Supplemental Figure 7. Patterns of *rps7-ndhB*, *psaC-ndhD*, and *rpoB* transcripts. Total RNA (5 μg) isolated from leaves of 4-week-old *crr22-1*, *crr22-1+CRR22DYW2*, *crr28-1*, and *crr28-1+CRR28DYW2* were analyzed by RNA gel blot hybridization. The arrows point at the mature transcript. The positions of RNA size markers are indicated at left. *crr22-1+CRR22DYW2*, *crr22-1* transformed with CRR22, in which the DYW motif was replaced by that of CRR2; *crr28-1+CRR28DYW2*, *crr28-1* transformed with CRR28, in which the DYW motif was replaced by that of CRR2.

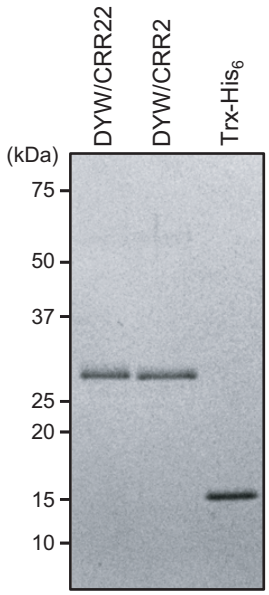

Supplemental Figure 8. Purified recombinant proteins used in this study. All proteins were expressed as native forms. The proteins were purified and analyzed by SDS-PAGE (10-20% gradient gel) and Coomassie Brilliant Blue. Three hundred nanograms of protein were loaded in each lane.

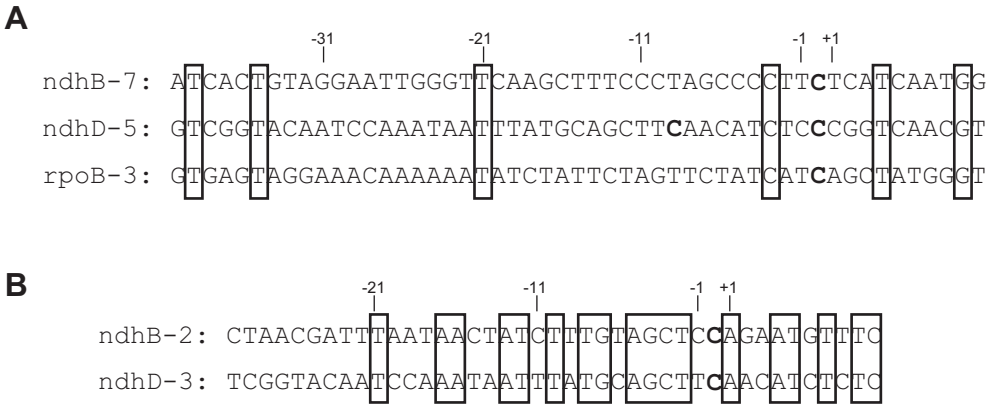

Supplemental Figure 9. Comparison of the nucleotide sequences in the regions surrounding the editing sites affected in *crr22* and *crr28*. (A) Sequence alignment of the region surrounding ndhB-7, ndhD-5, and rpoB-3 editing sites. The alignment includes the sequence from -40 to +10 around the edited C (bold letter) with identical nucleotides shown by boxes. **(B)** Sequence alignment of the region surrounding ndhB-2, and ndhD-3 editing sites. The alignment includes the sequence from -30 to +10 around the edited C (bold letter) with identical nucleotides shown by boxes.

Supplemental Table 1. Comparison of chloroplastic transcripts abundance

	clb19 com	*crr21*	WT	*ptac2*	*clb19*	*crr2*	*crr28*	*crr22*	*crr4*
psbA	-0.38125	-0.14705	0	-3.8779	-4.57567	-0.67397	-0.41997	-0.71136	-0.81133
matK	0.671019	0.08202	0	0.124091	0.553087	0.25415	0.339983	-0.2641	1.484087
rpS12A	0.074942	-0.28521	0	-0.94179	-0.2215	-0.4532	-0.2632	0.198711	0.645355
psbK	0.427897	-0.24209	0	-1.65544	-1.58963	0.132385	0.056378	0.333913	-0.12488
psbI	-0.32925	-0.2343	0	-1.66793	-1.46278	0.272833	0.186379	-0.03754	-0.25542
atpA	-0.09327	-0.14593	0	0	-0.04168	0.071723	0.413949	0.102194	-0.30753
atpF	0.181563	-0.2213	0	-0.89919	-0.8319	0.074549	0.283737	0.166897	-0.13843
atpH	0.509303	0.093735	0	-0.53696	-0.43326	0.188153	0.147679	-0.01748	-0.03118
atpI	0.296769	0.21967	0	-0.05971	0.112962	-0.04439	0.176054	0	-0.14002
rpS2	-0.00512	0.411275	0	1.7392	2.3521	0.080286	0.368717	-0.02673	0.011362
rpoC2	0.071436	0.762842	0	2.246464	2.943508	0.470615	0.5924	0.103809	0.757141
rpoC1	-0.30467	0.107867	0	2.386763	3.111502	0.075775	0.099081	0.401907	-0.35292
rpoB	0.037081	0.309326	0	1.561543	2.329089	-0.0091	0.179285	-0.00344	0.290118
petN	-0.14873	-0.49599	0	-1.40701	-1.06757	-0.24438	-0.4855	-0.47037	-0.41972
psbM	0.221208	-0.72134	0	-1.31095	-1.82626	-0.13643	-0.24209	-0.40592	-0.63194
psbD	-0.08933	-0.00493	0	-1.40386	-2.22861	-0.27958	0.012537	-0.17239	-1.25433
psbC	-0.17308	0.171566	0	-1.7116	-4.60719	0.015179	-0.12805	0.01859	-0.67392
psbZ	-0.04097	-0.30711	0	-2.12995	-3.0276	0.014008	0	-0.1392	-0.3782
rps14	-0.19901	0.15104	0	0.26234	-0.44375	0.301574	0.037828	-0.20308	-0.04386
psaB	0.1589	0.302381	0	-1.73207	-1.52257	0.223282	0.328701	0.415821	-0.47759
psaA	0.083826	0.563788	0	-1.85385	-1.81324	0.251565	0.365921	0.486458	-0.56606
ycf3	-0.05335	0.008775	0	-0.95562	0.377306	-0.04325	1.052007	-0.42267	1.208809
rps4	0.152839	0.011478	0	1.101467	1.596025	-0.00514	0.32226	-0.22848	0.411232
ndhJ	-0.43084	-0.74484	0	0.605819	0.092139	-0.06037	0.083444	0.120421	-0.3152
ndhK	-0.23067	-0.56226	0	0.446139	0	-0.00917	0.10537	0.210195	-0.31027
ndhC	-0.30827	-0.39026	0	0.346067	0.017382	0.168074	0.379449	0.128164	-0.07792
atpE	-0.10356	-0.37714	0	0.44481	0.76751	-0.14723	-0.15808	-0.31277	0.166729
atpB	-0.00753	-0.22791	0	0.419167	0.55861	-0.03307	-0.09224	-0.17452	0.210903
rbcL	0.265241	-0.06364	0	-3.09319	-2.98438	0.038422	0.05315	-0.18225	0.095623
accD	0.419467	0.93634	0	1.773232	1.403921	-0.0981	0.180863	0.367384	0.255014
psaI	0.182635	-0.22337	0	-0.22	-0.02555	-0.00911	0.095467	0.033771	-0.5321
ycf4	0.324215	0.067878	0	0.160222	0.434774	0.075215	0.337705	0.285886	-0.20653
cemA	0.308141	-0.04881	0	0.245092	0.190068	-0.06729	0.544942	0.231123	-0.16338
petA	0.093455	0.087155	0	0.236524	0.129564	-0.16575	0.274886	0.120332	0.18341
psbJ	-0.05824	0.180033	0	-0.31487	-0.43318	0	-0.22618	-0.51979	0.119915
psbL	0.098901	-0.27597	0	-1.89654	-2.20932	-0.25733	-0.66073	-0.24499	-0.26296
psbF	0.108163	-0.28141	0	-2.02175	-2.28457	-0.30071	-0.47084	-0.13086	-0.01192
psbE	0.014451	-0.05347	0	-2.73972	-2.81749	-0.03415	-0.52213	-0.20322	-0.08725
petI	-0.14677	-0.19595	0	-0.42739	-0.59631	-0.40411	-0.44525	-0.15135	0.239166
petG	-0.89175	-0.2404	0	-0.64021	-0.61463	-0.34444	-0.36815	-0.18852	0.219649
psaJ	0.222831	-0.10214	0	-1.86917	-1.96043	0.041747	-0.16982	-0.50234	0.41297
rpL33	0.251907	0.000983	0	2.126871	1.799208	-0.37604	0.2385	-0.2442	-1.5403
rpS18	-0.00039	0.007525	0	2.620379	2.664124	-0.23754	-0.05371	0.000145	-0.76698
rpL20	-0.27397	-0.04246	0	2.303254	2.710002	-0.07961	-0.03773	0.165935	-0.22051
clpP1	0	0.195672	0	0.47484	1.427224	-0.42206	-0.10212	0.463934	0.061215
psbB	0.263667	0.063854	0	-1.79702	-1.60573	0.010932	-0.19152	-0.13256	-0.26908
psbT	0.165803	0.143095	0	-1.52063	-1.6223	0.294348	0.159697	0.016366	-0.266
psbN	-0.4514	0.156777	0	-3.21194	-3.34212	-0.16796	-0.08396	-0.45128	-0.53972
psbH	0.396272	0.03559	0	-2.68629	-2.70398	0.057436	0.169413	0.107329	-0.12235
petB	0.287102	-0.01252	0	-1.30776	-1.41211	-0.31248	-0.15551	-0.22931	-0.36083
petD	0.081309	-0.04154	0	-1.99376	-1.80762	-0.15841	-0.11159	-0.39164	-0.23071
rpoA	0.335677	0.399541	0	1.531229	2.027805	0.246353	-0.07601	0.293778	0.180423
rpS11	0.22911	0.279179	0	1.588512	2.131779	0.216992	0.006112	0.206499	0.248139
rpL36	0.121849	0.195948	0	1.704809	2.041811	0.374138	-0.03358	0.133785	0.267518
rpS8	0.142118	0.34107	0	1.50758	1.981663	0.413704	-0.12018	0.174237	0.415669
rpL14	0.439935	0.183462	0	1.461706	1.769387	0.43001	-0.05975	0.061445	0.516808
rpL16	0.056062	0.291559	0	1.320629	1.762046	0.33362	-0.16031	0.062178	0.73677

rpS3	0.291576	0.389402	0	1.278306	1.795297	0.486295	0.026474	0.023691	0.807895
rpL22	0.491369	0.184881	0	1.5842	1.630596	0.286208	0.339009	0.023903	1.16045
rpS19	-0.08635	0.154861	0	0.99929	1.556277	0.1142	0.004283	-0.12605	1.062649
rpL2	0.314834	-0.33038	0	0.529462	0.804339	0.08583	-0.23603	0.009119	0.334961
rpL23	0.269965	0.021103	0	0.578327	0.708685	0.292943	-0.03088	0.128508	0.392572
ycf2.1	-0.16834	0.12604	0	1.699755	1.587179	0.127957	0.244022	0.229436	0.881938
ycf15	-0.29407	0.11647	0	1.49369	1.69659	0.310014	0.07626	-0.02416	1.248631
ndhB	0.003708	-0.39523	0	1.098768	0.437822	-0.65445	-0.09221	0.087187	0.465247
rpS7	-0.02688	0.061374	0	1.211729	1.279704	-0.37696	-0.09157	0.32785	0.237227
ycf1	0.163605	-0.26711	0	1.341033	0.764235	0.327667	0.360155	0.361365	0.522341
ndhF	-0.13706	0.189725	0	0.264457	-0.20554	0.341312	0.468212	0.676297	0.190206
rpL32	0.342982	-0.50708	0	1.212828	1.541495	-0.20337	-0.46186	0.069544	0.128561
ccsA	0.033335	0	0	1.654077	1.518438	0.294156	-0.28024	-0.23497	0.238918
ndhD	0.215151	0.206616	0	0.883917	1.037706	0.653851	0.534861	-0.18681	0.353621
psaC	-0.03317	-0.45609	0	-0.25472	-0.76016	0.368134	-0.02835	-0.0211	0
ndhE	-0.12823	-0.32127	0	-0.75745	-1.13218	-0.06022	0.377882	0.03196	0.02767
ndhG	-0.23877	-0.02818	0	-0.15552	-0.67299	0.101225	0.472589	0.233858	0.065162
ndhI	-0.02907	0.084631	0	0.101314	-0.31914	-0.10346	0.602739	0.22511	-0.13776
ndhA	-0.21574	0.138724	0	-2.74413	-4.92625	0.206829	0.393505	0.124265	-0.00708
ndhH	-0.24999	0.22468	0	2.165984	1.755051	-0.02338	0.551369	0.15399	-0.10225
rpS15	-0.19019	0.11887	0	2.270055	2.571506	-0.00273	-0.06427	-0.19332	0.81204
18S	-0.22976	-0.59274	0	-0.25311	-0.01346	-0.44106	-0.33605	-0.84764	-0.37712
QC16S	-0.47486	-0.25898	0	-2.6706	-3.10477	-0.22244	-0.3217	-0.4965	-0.30674
QC23S	-0.43732	-0.28219	0	-2.1595	-1.22693	0.011775	-0.46911	-0.11401	1.385455

Supplemental Table 2. Oligonucleotide primers used

name	sequence
For generating PCR templates for PPE assay	
ndhDATfor:	CAAGCCTAATTCTATCATAACTCG
ndhDATrev:	AAGTTTATATGGTTCGAACG
ndhBedIII:	ATTTCTTGAAGCTCAATCTCTCCCCCGGAT
ndhBfor2:	TCATGATCTGGCATGTACAG
Nb11:	TTCATGCTTGTTTGAGTAATAGC
p12.AT:	GATCTAATGAGGCTACTATG
rpoBATfor:	GAAAACCAGTAGGAATATGC
rpoBATrev:	GTCTCCAATTAATATTTCGGCG
For PPE assay	
ndhD(116290)_PPE_C:	AGTCGGTACAATCCAAATAATTTATGCAGC
ndhD(116281)_PPE_A:	GCTATTCTCTTTTTTAAATTACGTTGA
ndhB(96998)_PPE_C:	CTAACGATTTAATAACTATCTTTGTAGCTC
ndhB(96419)_PPE_C:	AGGAATTGGGTTCAAGCTTTCCCTAGCCCC
rpoB(25779)_PPE_C:	GTAGGAAACAAAAAATATCTATTCTAGTTC
For HRM analysis	
matK_HRM_for:	TGAATCCAAGATTTTTCTTGTTCTT
matK_HRM_rev:	AAAAAGATGGATTCGTATTCACA
atpF_HRM_for:	GCCGGGAGTTTCGGATTTA
atpF_HRM_rev:	GATCAATACACCGAAAACTACACTT
rpoC1_HRM_F:	TTCTTTTGCTAGGCCCATAA
rpoC1_HRM_R:	TGCTGTATTTCCAGGATTGAA
rpoB23898_HRM_for:	TGGTTCAAGTTATAACCCAGAAAT
rpoB23898_HRM_rev:	CCATGTCTTCCAGCTACTTTATCA
rpoB25779_HRM_for:	GCTCGGGTGAGTAGGAAACA
rpoB25779_HRM_rev:	TCTAGAATTTCTCGTAGATTCAAACC
rpoB25992_HRM_for:	TCCTTTAATGAATTCCCTTGGA
rpoB25992_HRM_rev:	CGGGACTTTGCAATATTTGAT
psbZ_HRM_for:	TGCTTTCCAATTGGCAGTTT
psbZ_HRM_rev:	GAGACGCAAATACAACGGGTA
RPS14(37092)HRM_for:	TCGCTAAGTGAGAAATGGAAAA

RPS14(37092)HRM_rev:	CGTCGATGAAGACGTGTAGG
RPS14(37161)HRM_for:	GAAGAAGAGGCAAAAATTGGAA
RPS14(37161)HRM_rev:	TTCTCACTTAGCGACGGAATC
accD_HRMfor:	TGAATGTTTGTGAACAATGTGG
accD_HRMrev:	GATTCCAAGTACCCGGATCA
accD(58642)HRM_rev:	ACTTTTTAGCTTGTTGATAGAGGTTT
accD(58642)HRM_for:	GCATTTTTCTTTCAAATCATTTTT
psbF_HRM_rev:	TCGTTGGATGAACTGCATTG
psbF_HRM_for:	GGCTGTTCATGGACTAGCTGTA
psbE_HRM_rev:	TGGGTCCTCCTAAAAAGATCTAC
psbE_HRM_for:	AAGGCATTCCATTAATAACAGG
petL_HRM_for:	ATTTTATTGAGTCCCTTCATGC
petL_HRM_rev:	AAAGCTGCTAGTAGAAAACCGAAA
Rps12_HRM_rev:	TCGAGTTCGTCCATTCTATTTT
Rps12_HRM_for:	AGACTGAGACATAAAAAGGAAATTCT
clpPAt2rev:	TGAACCGCTACAAGATCAAC
clpP_HRM70for:	GAAGACATGGAACGGGATGT
rpoA_HRMfor:	TTGGCGAAATAGAAGGAACA
rpoA_HRMrev:	CCTGCTATGTTAGAATAGTCATGTGG
Rpl23_HRM_r:	GAAGAGTTCGACCCAATGCT
Rpl23_HRM_f:	TCAATATACTTTTAATGTCGAATCAGG
ndhB(94999)HRM_for:	TTCCATCGAATTGAGTATGATTG
ndhB(94999)HRM_rev:	AATCGCAATAATCGGGTTCA
ndhB95225_HRM_for:	GGTCTTCCTCCACTAGCAGGT
ndhB95225_HRM_rev:	CTGCCATCCACACCAGAATA
95640R:	CACTCGAATTTTCGATATTCCTTT
ndhB(95608)HRM_rev:	TCCAGAAGAAGATGCCATTCA
95618F:	AAGGAATATCGAAAATTCGAGTGG
95693R:	CCAGTCGTTGCTTTTCTTTCTG
95627F:	CGAAAATTCGAGTGGCTGA
95698R:	CCACTCCAGTCGTTGCTTTT
96461R:	TCATCACTGTAGGAATTGGGTTC
ndhB(96419)HRM_rev:	CTTCGTATACGTCAGGAGTCCA
96606R:	GGTGGGGCAAGCTCTTCTAT
96537F:	CAATCTCTCCCCCGGATG
ndhB(96698)HRM_for:	TTTTTATGTGGTGCTAACGATTT

ndhB(96698)HRM_rev:	CCAGATAATAGGTAGGAGCATAAACTG
ndhB(97016)HRM_for:	TTGGCCTAATTCTTCTTCTGATG
ndhB(97016)HRM_rev:	TTGAAGAGATGAAATATAACCAAGG
ndhF(112349)HRM_for:	TTCGGTTACTTTATCGATCCAC
ndhF(112349)HRM_rev:	TCAGAACCAAAATCCCAACAG
116318R:	GGTACAATCCAAATAATTTATGCAG
116228F :	CCATATGAGATACAGAAGAATAGGC
ndhD(116494)HRM_for:	TTGGATTTCTTATTGCTTTTGC
ndhD(116494)HRM_rev:	CACCGTGGGTGTCAGGTAAC
ndhD(116785)HRM_for:	AGCAATGTACAGCGGTCAAA
ndhD(116785)HRM_rev:	TTCTAATTCCCACATGATGAAAAA
ndhD(117166)HRM_for:	TTGGACCTGGTGTATCTTGTC
ndhD(117166)HRM_rev:	CCAGCAGATATTGGAAAAACAA
ndhG_HRMfor:	TTGCCTGGACCAATACATGA
ndhG_HRMrev:	CACTCCCAGACCCCCTACTA

For analysis of RNA editing in transgenic plants

ndhB-FW:	TGCTTCTCTTCGATGGAAG
ndhB-RV:	TCCTTCGTATACGTCAGG
ndhB-FW2:	TCCCACTCCAGTCGTTG
ndhB-RV2:	TGAGCAATCGCAATAATCG
ndhD-FW:	AGTACGCGTTCTTTGGAC
ndhD-RV:	TAGCTCCATTAAGTCCAGG
rpoB-FW:	TCAATTGGTAGAACCTCTG
rpoB-RV:	TATTTCGGCGACCAATCC

For RNA gel blot analysis

ndhB-exon-FW:	TCTCCCACTCCAGTCGTTG
ndhB-exon-RV:	TGAGCAATCGCAATAATCGG
ndhD-FW:	TTCTTCTAACGACCTACGC
ndhD-RV:	TAATCGGTGATTTGACGGC
rpoB-FW:	AGGGAACATCTGCAATACC
rpoB-RV:	CTCCTTATCGGTCAAGAAAG

For construction of pT-DYW2 and pT-DYW22

CRR2_H4-F:	GGGAGATCTCTTGGTTCTTGTAGAATTCACGG

CRR2_F-R:	GGGGTCGACCCAGTAATCTCCACAAGAACAC
DYW22-OX-FW:	GAAGCTGGTTATGTTCCTG
DYW22-OX-RV:	CCAGTAATCTCCGCACG

Preparation of template DNA for *in vitro* transcription

NB2-F:	ATGTAATACGACTCACTATAGGGGTTATATTTCATCTCTTCAA CAAG
NB2-R:	CCCATAGGGGCATAAACTGAAACATTCTGGAGC

Supplemental Methods

Chlorophyll Fluorescence Analysis

Chlorophyll fluorescence was measured with a MINI-PAM portable chlorophyll fluorometer (Walz, Effeltrich, Germany) in ambient air at room temperature (25^{o}C). Minimum fluorescence at open PSII centers in the dark-adapted state (*Fo*) was excited by a weak measuring light (wavelength 650 nm) at a PFD of 0.05-0.1 μmol m^{-2} s^{-1}. A saturating pulse of white light (800 ms, 3,000 μmol photons m^{-2} s^{-1}) was applied to determine the maximum fluorescence at closed PSII centers in the dark-adapted state (*Fm*) and during AL illumination (*Fm'*). The steady state fluorescence level (*Fs*) was recorded during AL illumination (15-1,000 μmol photons m^{-2} s^{-1}). These photosynthetic parameters were determined 2 min after the change of AL intensity. NPQ was calculated as (*Fm-Fm'*)/*Fm'*. The quantum yield of PSII (ϕ_{PSII}) was calculated as (*Fm'-Fs*)/*Fm'* (Genty et al., 1989). ETR was calculated as ϕ_{PSII}xPFD. The transient increase in chlorophyll fluorescence after AL had been turned off was monitored as described (Shikanai et al., 1998).

RNA preparation and RNA gel blot analysis

For Supplemental Figure 2, RNA preparation and RNA gel blot were performed as follows. Total RNA was isolated using a plant RNeasy kit (Qiagen, Valencia, CA). Ten micrograms of RNA (15 micrograms for *rpoB*) was loaded on formaldehyde agarose gels and transferred onto Hybond N+ nylon membrane (GE Healthcare, Piscataway, NJ). RNA integrity, loading and transfer were checked by staining the membrane with methylene blue. Hybridizations were performed under high-stringency conditions using antisense RNA probes internally labeled with biotinylated cytidine. The probes were synthesised by cloning PCR products in pGEM-T Easy vector (Promega, Madison, WI). The primers used for the PCR were rpoB.AT.for (GAAAACCAGTAGGAATATGC) and rpoB.AT.rev (GTCTCCAATTAATATTTCGGCG), ndhB.AT.rev2 (CTAAAAAAGGGTATCCTGAGC) and AndhB (GTCGTTGCTTTTCTTTCTG) corresponding to the 2nd exon of *ndhB*, and chloro 213 F (AATAGTATTTCAAGTGTAACAGGATAGGA) and chloro 213R (TGGACGATCCATTAATTCAACT) for *ndhD*. Clones with inserts in antisense orientation were amplified by PCR using the forward primer and M13/pUC reverse (GAGCGGATAACAATTTCACACAGG). The PCR products served as a template for *in vitro* transcription with SP6 polymerase following the manufacturer's recommendations (Maxiscript Ambion). Signal detection was performed using the

Phototope Star detection kit (New England Biolabs, Ipswich, MA) and read in a LAS-1000 (FujiFilm). The arrows point at the mature transcript. Sizes of RNA markers (Promega) are shown in kilobases.

For Supplemental Figure 7, the fragments used as probes were obtained by PCR amplification using the oligonucleotides 5'-TCTCCCACTCCAGTCGTTG-3' and 5-TGAGCAATCGCAATAATCGG-3' for *ndhB* and the oligonucleotides 5'-TTCTTCTAACGACCTACGC-3' and 5'-TAATCGGTGATTTGACGGC-3' for *ndhD*. Labeling of the probe was carried out by using a PCR DIG Probe Synthesis Kit (Roche, Indianapolis, IN). Total RNA was isolated from the leaves of 4-week-old plants by using an RNeasy Plant Mini Kit (Qiagen) and treated with DNase I (Invitrogen, Carlsbad, CA). Total RNA (5 μg) was then loaded onto a 1% agarose gel containing 0.6 M formaldehyde and electrophoresed in 1xMops buffer (pH 7.0) comprising 20 mM Mops, 5 mM sodium acetate, and 2 mM EDTA. After electrophoresis, the RNA was transferred onto a nylon membrane and hybridized with DIG-labeled DNA probe. The signals from the hybridized bands were detected by using a Gene Image CDP-Star Detection Kit (GE Healthcare).

Analysis of chloroplast transcripts and clustering

Chloroplast transcript accumulation was analysed as described (Chateigner-Boutin et al., 2008). The profiles corresponding to the various samples analysed (see Supplemental Table 2) were clustered with Avadis Prophetic 4.3 (Strand Life Sciences) using the $\log_2$ value of the mutant/WT ratios after normalization by setting the median of the ratios to 0 for each sample. The euclidian distances between the samples were then calculated and the dendrogram was drawn by hierarchical clustering using the complete linkage rule (D'haeseleer, 2005).

Constructs and Plant Transformation

For complementation of the *crr22* and *crr28* mutations, the wild-type genomic sequence delimited by 5'-CCTCCAATTCTTGCGTTTG-3' and 5'-TCACCAGTAATCTCCGCAC-3' including the *CRR22* coding region and by 5'-GAGAAGGACTTGATGAGG-3' and 5'-CTACCAGTAGTCTAAACAAG-3' including the *CRR28* coding region were cloned into pGWB-NB1 binary vector. The resultant plasmids were introduced into *crr22-1* and *crr28-1* via *Agrobacterium tumefaciens* ASE.

For the expression of CRR2, CRR22, and CRR28 lacking their DYW motifs to be deleted, the wild-type genomic sequences surrounded by 5'-

TCTCCATGAAAGCCATCC -3’ and 5’-CAATCGGCTTCTATACTTC-3’ for CRR2, 5’- CCTCCAATTCTTGCGTTTG -3’ and 5’-TTTGATGTGGCATATCAGCTTC-3’ for CRR22, and by 5’- GGAGAAGGACTTGATGAGG -3’ and 5’-TCTTAGCCTGTCGTCGATC-3’ for CRR28 were cloned into the pGWEB-NB1 binary vector fusing the HA-tag at the C-terminus. The resultant plasmids were introduced into *crr2-1, crr22-1,* and *crr28-1* via *Agrobacterium tumefaciens* ASE.

For the expression of CRR22 and CRR28 lacking their E and DYW motifs, the wild-type genomic sequences delimited by 5’- CCTCCAATTCTTGCGTTTG -3’ and 5’-CAATCTCTCTGCTGCTTTC-3’ for *CRR22* and by 5’-GAGAAGGACTTGATGAGG -3’ and 5’-AATATTTCTAGCAATTTCTTCAC-3’ for *CRR28* were cloned into the pGWEB-NB1 binary vector fusing the HA-tag at the C-terminus. The resultant plasmids were introduced into *crr22-1* and *crr28-1* via *Agrobacterium tumefaciens* ASE.

For the expression of CRR2, in which the DYW motif of CRR2 is replaced by that of CRR22 or CRR28, the wild-type genomic sequence delimited by 5’-TCTCCATGAAAGCCATCC-3’ and 5’-CTTCATATCTTCGGCTAAC-3’ was amplified by PCR and was ligated to the sequence encoding the DYW motif of CRR22 delimited by 5’-GAAGCTGGTTATGTTCCTG-3’ and 5’- CCAGTAATCTCCGCACG -3’ or the sequence encoding the DYW motif of CRR28 delimited by 5’-TCAATTGGTTATTTACCGGATG-3’ and 5’- CCAGTAGTCTAAACAAGAGC-3’. The resultant chimeric genes were cloned into the pBIN19 binary vector fusing the HA-tag at the C-terminus. The resultant plasmids were introduced into *crr2-1* via *Agrobacterium tumefaciens* MP90.

For the expression of CRR22, in which the DYW motif of CRR22 is replaced by that of CRR2 or CRR28, the wild-type genomic sequence delimited by 5’-CCTCCAATTCTTGCGTTTG -3’ and 5’- TTTGATGTGGCATATCAGCTTC -3’ was amplified by PCR and was ligated to the sequence encoding the DYW motif of CRR2 delimited by 5’-GAGAAAGGGTACATACCAC-3’ and 5’-CCAGTAATCTCCACAAGAAC-3’ or the sequence encoding the DYW motif of CRR28 delimited by 5’- TCAATTGGTTATTTACCGGATG -3’ and 5’-CCAGTAGTCTAAACAAGAGC -3’. The resultant chimeric genes were cloned into the pGWB-NB1 binary vector fusing the HA-tag at the C-terminus. The resultant plasmids were introduced into *crr22-1* via *Agrobacterium tumefaciens* ASE.

For the expression of CRR28, in which the DYW motif of CRR28 is replaced by that of CRR2 or CRR22, the wild-type genomic sequence surrounded by 5’-GGAGAAGGACTTGATGAGG -3’ and 5’- TCTTAGCCTGTCGTCGATC -3’ was

amplified by PCR and was ligated to the sequence encoding the DYW motif of CRR2 delimited by 5'- GAGAAAGGGTACATACCAC -3' and 5'- CCAGTAATCTCCACAAGAAC -3' or the sequence encoding the DYW motif of CRR22 surrounded by 5'- GAAGCTGGTTATGTTCCTG-3' and 5'- CCAGTAATCTCCGCACG -3'. The resultant chimeric genes were finally cloned into the pGWB-NB1 binary vector fusing the HA-tag at the C-terminus. The resultant plasmids were introduced into *crr28-1* via *Agrobacterium tumefaciens* ASE.

Supplemental References

Chateigner-Boutin, A.L., Ramos-Vega, M., Guevara-Garcia, A., Andrés, C., de la Luz Gutiérrez-Nava, M., Cantero, A., Delannoy, E., Jiménez, L.F., Lurin, C., Small, I., and León, P. (2008). CLB19, a pentatricopeptide repeat protein required for editing of *rpoA* and *clpP* chloroplast transcripts. Plant J. **56:** 590-602.

Pfalz, J., Liere, K., Kandlbinder, A., Dietz, K.J., and Oelmuller, R. (2006). pTAC2, -6, and -12 are components of the transcriptionally active plastid chromosome that are required for plastid gene expression. Plant Cell **18:** 176-197.

de Longevialle, A.F., Hendricson, L., Taylor, N.L., Delannoy, E., Lurin, C., Badger, M., Millar, A.H., and Small, I. (2008). The pentatricopeptide repeat gene *OTP51* with two LAGLIDADG motifs is required for the *cis*-splicing of plastid *ycf3* intron 2 in *Arabidopsis thaliana*. Plant J. **56:** 157-168.

Genty, B., Briantais, J.M., and Baker, N.R. (1989). The relationship between the quantum yield of photosynthetic electron-transport and quenching of chlorophyll fluorescence. Biochim. Biophys. Acta **990:** 87-92.

Shikanai, T., Endo, T., Hashimoto, T., Yamada, Y., Asada, K., and Yokota, A. (1998). Directed disruption of the tobacco *ndhB* gene impairs cyclic electron flow around photosystem I. Proc. Natl. Acad. Sci. USA **95:** 9705-9709.

D'haeseleer, P. (2005). How does gene expression clustering work? Nat. Biotechnol. **23:** 1499-1501.